Chapter 2

PROGRAMMING MODELS AND RUNTIMES

Georges Da Costa[1] *and Alexey L. Lastovetsky*[2] *and Jorge G. Barbosa*[3] *and Juan C. Díaz-Martín*[4] *and Juan L. García-Zapata*[5] *and Matthias Janetschek*[6] *and Emmanuel Jeannot*[7] *and João Leitão*[8] *and Ravi Reddy Manumachu*[9] *and Radu Prodan*[10] *and Juan A. Rico-Gallego*[11] *and Peter Van Roy*[12] *and Ali Shoker*[13] *and Albert van der Linde*[14]

Keywords: Performance Modelling, Energy Modelling, Heterogeneous Platforms, Optimization Techniques, Cloud Computing; Edge Computing; Process Placement; Graph Partition; Sustainability; Energy awareness; Availability; Scalability.

Several millions of execution flows will be executed in Ultrascale Computing Systems (UCS), and the task for the programmer to understand their coherency and for the runtime to coordinate them is unfathomable. Moreover, in link with USC large scale and their impact on reliability the current static point of view is not more sufficient. A runtime cannot consider to restart an application because of the failure of a single node as statically several nodes will fail every days. Classical management of these failures by the programmers using checkpoint-restart are also too limited due to the overhead at such scale.

[1]University of Toulouse, France
[2]University College Dublin, Ireland
[3]Faculdade de Engenharia da Universidade do Porto, Portugal
[4]University of Extremadura, School of Technology, Spain
[5]University of Extremadura, School of Technology, Spain
[6]Institute of Computer Science, University of Innsbruck, Austria
[7]INRIA Bourdeaux Sud-Ouest, LaBRI, Université de Bourdeaux, France
[8]Universidade Nova de Lisboa, Portugal
[9]University College Dublin, Ireland
[10]Institute of Information Technology, University of Klagenfurt, Austria
[11]University of Extremadura, School of Technology, Spain
[12]Université Catholique de Louvain, Belgium
[13]HASLab, INESC TEC & University of Minho, Portugal
[14]Universidade Nova de Lisboa, Portugal

Emerging programming models that facilitate the task of scaling and extracting performance on continuous evolving platforms, while providing resilience and fault tolerant mechanisms to tackle the increasing probability of failures throughout the whole software stack, are needed to achieve scale handling (optimal usage of resources, faults), improve programmability, adaptation to rapidly changing underlying computing architecture, data-centric programming models, resilience, energy efficiency.

One key element on the ultrascale front is the necessity of new sustainable programming and execution models in the context of rapid underlying computing architecture changing. There is a need to explore synergies among emerging programming models and runtimes from HPC, distributed systems and big data management communities. To improve the programmability of future systems, the main changing factor will be the substantially higher levels of concurrency, asynchrony, failures and heterogeneous architectures.

UCS need new sustainable programming and execution models, suitable in the context of rapidly changing underlying computing architecture, as described in [7]. Advances are to be expected at three levels: Innovative programming models with higher level abstraction of the hardware; breakthrough for more efficient runtimes at large scale; cooperation between the programming models and runtime levels.

Furthermore all the programming ecosystem must evolve. A large number of scientific applications are built on the message passing paradigm which needs a global point of view during the programming phase and usually require global synchronization during execution. But even at lower granularity, classical libraries must evolve. As an example, a large number of scientists use the linear algebra BLAS libraries for their optimized behavior on current supercomputers. Improving the performance of this library on UCS would prove largely beneficial.

This chapter explores programming models and runtimes required to facilitate the task of scaling and extracting performance on continuously evolving platforms, while providing resilience and fault-tolerant mechanisms to tackle the increasing probability of failures throughout the whole software stack. However, currently no programming solution exists that satisfies all these requirements. Therefore, new programming models and languages are required towards this direction. The whole point of view on application will have to change. As we will show, the current wall between runtime and application models leads to most of these problem. Programmers will need new tools but also new way to assess their programs. Also, data will be a key concept around which failure-tolerant high number of micro-threads will be generated using high-level information by adaptive runtime. One complex element comes from the difficulty to test these approaches as UCS systems are not yet available. Most of the following explorations are extrapolated to UCS scale but only actually proven an currently existing infrastructure.

The complexity of UCS computing architecture integrating in a hierarchical heterogeneous way multicore CPUs and various accelerators makes many traditional approaches to the development of performance and energy efficient applications ineffective. New sustainable approaches based on accurate and sustainable application-level performance and energy models have a great potential to improve the performance and energy efficiency of applications and create a solid basis for the emerging USC programming tools and runtimes. Section 2.1 of this chapter covers this topic by describing accurate models of the hardware and software usable during the design phase, but also means or reasoning on these models. With these tools, it becomes possible to adapt and tune finely applications during the design phase to run efficiently on large scale heterogeneous platforms.

Optimizing UCS usage is difficult due to the large number of possible use-cases. In particular ones such as Scientific workflow, it becomes possible to use a dedicated abstraction. As scientific workflow scheduling for UCS is a major challenge, the impact of proposing a particular abstraction along-with dedicated runtime harnessing the particularities of this abstraction leads to a high improvement of the efficiency of using a UCS. The approaches to solve this challenge are covered in section 2.2. In this section, both the *Abstract part* (linked with the design and programming of the workflow) and the *Concrete part* (linked with its actual scheduling and execution) are described. This specific high-level abstraction shows that link between programming models and runtime helps to simplify the task of programmers to harness the power of the underlying large scale heterogeneous systems.

With the emergence of UCS, a new computing revolution is coming: Edge computing. Instead of harnessing computing power directly from large scale datacenters, new proposal comes from the possibility to interconnect and coordinate large number of distributed computing nodes. Due to the explosion of IoT applications the aggregated Edge computing power is increasing extremely fast. These two systems (Edge and UCS) share the difficulty to manage large number of distributed execution flows in a dynamic and heterogeneous environment. These similarities is explored in Section 2.3 where key elements of programming models and runtime for large scale Edge computing are explored.

Due to the scale of UCS, even classical management operation of the platform becomes complex. As an example, section 2.5 shows how a simple operation such as graph partitioning becomes complex at large scale. This operation is central in the management of a platform as it is needed to minimize communication between nodes when used for placing the tasks. In this section several challenges are addressed such as the scale but also the heterogeneity of tasks, computing nodes and networking infrastructure.

This chapter concludes with a description of the main global challenges linked to programming models, runtimes and the link between these two as described in NESUS roadmap[6].

2.1 Using Performance and Energy Models for Ultrascale Computing Applications

Ultrascale systems, including high performance computing, distributed computing and big data management platforms, will demand a huge investment of heterogeneous computing and communication equipment. Ensuring the availability of current and future social, enterprise and scientific applications with efficient and reliable execution on these platforms remains nowadays an outstanding challenge. Indeed, reducing their power footprint while still achieving high performance has been identified as a leading constraint in this goal. Model-driven design and development of optimal software solutions should play a critical role in that respect.

Energy consumption is one of the main limiting factors for designing and deploying ultrascale systems.

Using monitoring and measurement data, Performance and Energy models contribute to quantify and gain insights into the performance and power consumption effects of system components and their interactions, including both hardware and the full software stack. Analysis of the information provided by the models is then used for tunning applications and predicting its behavior under different conditions, mainly at scale.

This chapter describes methods, facilities and tools for building performance and energy models, with the goal of aiding in the design, development and tunning of data-parallel and task-parallel applications running on complex heterogeneous parallel platforms.

2.1.1 Terminology

In this section, we describe the various terms related to power and energy predictive models used in this work.

There are two types of power consumptions in a component: dynamic power and static power . Dynamic power consumption is caused by the switching activity in the component's circuits. Static power is the power consumed when the component is not active or doing work. Static power is also known as idle power or base power. From an application point of view, we define dynamic and static power consumption as the power consumption of the whole system with and without the given application execution respectively. From the component point of view, we define dynamic and static power consumption of the component as the power consumption of the component with and without the given application utilizing the component during its execution respectively.

There are two types of energy consumptions, static energy and dynamic energy. We define the static energy consumption as the energy consumption of the platform without the given application execution. Dynamic energy consumption is calculated by subtracting this static energy consumption from the total energy consumption of the platform during the given application execution. That is, if P_S is the static power consumption of the platform, E_T is the total energy consumption of the platform during the execution of an application, which takes T_E seconds, then the dynamic energy E_D can be calculated as,

$$E_D = E_T - (P_S \times T_E) \tag{2.1}$$

2.1.2 Performance Models of Computation

In this section, we survey prominent models used for prediction of the cost of computations in the execution of ultrascale computing applications.

The seminal models are the parallel random access machine (PRAM) [8], the bulk-synchronous parallel model (BSP) [9], and the LogP model [10]. All these models assume a parallel computer to be a homogeneous multiprocessor.

The PRAM is the most simplistic parallel computational model . It consists of p sequential processors sharing a global memory. It assumes that synchronization and communication is essentially cost free. However, these overheads can significantly affect algorithm performance. Many modifications to the PRAM have been proposed that attempt to bring it closer to practical parallel computers.

The BSP model is a bridging model that consists of p parallel/memory modules, a communication network, and a mechanism for efficient barrier synchronization of all the processors. A computation consists of a sequence of supersteps. During a superstep, each processor performs synchronously some combination of local computation, message transmissions, and message arrivals.

Finally, LogP (covered later in much detail) abstracts the performance of a system with four parameters, L, o, g, and P, which stand for network delay, overhead or cycles that a CPU devotes to sending the message, gap per message or minimum time interval between two consecutive injections to the network, and, finally, number of processes. It has been successfully used for developing fast and portable parallel algorithms for (homogeneous) supercomputers and has become a foundation for numerous subsequent models.

A dominant class models parallel computation by Directed Acyclic Graph (DAG) where the nodes represent local computation and the edges signify the data dependencies. This model forms the fundamental building block of runtime schedulers in KAAPI [11], StarPU [12], and DAGuE [13].

Graphical models are commonly used to structure mesh-based scientific computations. The objective of a graph partitioning problem is then to divide the vertices of the graph into approximately equal-weight partitions (balance computations) and minimize the number of cut edges between partitions (minimize total runtime communication) [14], [15], [16], [17].

We will now review performance models of computation for heterogeneous platforms where they are even more paramount.

Performance Models of Computation for Heterogeneous HPC Platforms

Realistic and accurate performance models of computation are the fundamental building blocks of data partitioning algorithms. Over the years, load balancing algorithms developed for performance optimization on parallel platforms have attempted to take into consideration the real-life behavior of applications executing on these platforms. This can be discerned from the evolution of performance models for computation used in these algorithms.

The simplest models used positive constant numbers and different notions such as normalized processor speed, normalized cycle time, task computation time, average execution time, etc to characterize the speed of an application [18], [19], [20]. A common crucial feature of these efforts is that the performance of a processor is assumed to have no dependence on the size of the workload.

The most advanced load balancing algorithms use functional performance models (FPMs) , which are application-specific and represent the speed of a processor by continuous function of problem size but satisfying some assumptions on its shape [21],[22],[23],[24]. These FPMs capture accurately the real-life behaviour of applications executing on nodes consisting of uniprocessors (single-core CPUs).

Modern multicore platforms have complex nodal architectures with highly hierarchical arrangement and tight integration of processors where resource contention and Non-uniform Memory Access (NUMA) are inherent complexities. On these platforms, load balancing algorithms based on the traditional and state-of-the-art performance models (FPMs) will return sub-optimal solutions due to the complex nature of the performance models. Therefore, there is a need for novel performance models of computation that take into account these inherent complexities.

Lastovetsky et al. [25], [26] present an advanced performance model of computation (FPMs) that contains severe variations reflecting the resource contention and NUMA inherent in the modern multicore platforms. These models (or performance profiles) have complex shapes (non-linear, non-convex), which do not satisfy the assumptions on shape that allow load balancing algorithms based on smooth FPMs to return optimal workload distribution. The authors then propose data partitioning algorithms that use these advanced FPMs as building blocks to minimize the computation time of the parallel application.

2.1.3 Performance Models of Communications

This section fairly describes the issue of optimizing communication using analytical representations of the transmissions departing from a given workload balance of the computation between the processes of an application. We also introduce foundational analytical communication performance models and we apply one of the models to an example of a real-world kernel.

Ultra-scale Computer Systems are composed of heterogeneous multi-core processors and accelerators, connected by a hierarchy of communication channels. Such heterogeneity is partially due to the necessity of increasing the system performance keeping the energy cost at a reasonable level. Scientific applications executing on UCS platforms are composed of *kernels*, computationally intensive tasks conceived for being executed by a set of heterogeneous processors. Usually, every processor runs the same code on a different *data region* of a global data space. UCS applications face the challenge of obtaining as much performance as possible from the specific platform.

During execution of a kernel, each of the processes needs data from other processes to compute its own values. Therefore, the necessity of communication appears periodically during its execution. The challenge is not only to balance the overall computational load of the kernel among the available computing resources, but also to optimize the completion time of its communications.

Current approach is based on design and implement evaluation tests, execute them in the target platform, hence consuming computational resources along a significant amount of time, and extrapolate estimations obtained to the whole application. A model-based methodology replaces the previous test-based approach by a fully analytical modeling of the behavior of the application. Optimization of computation and communication in data parallel applications are usually addressed separately. First, computational load is distributed between processors according to their capabilities, following different approaches (see section 2.1.2). Then, communication optimization is addressed by building communication performance models and applying them for searching a distribution of the data space to the processes that reduces the communication cost.

A communication performance model provides with an analytic framework that represents communications as a parameterized formal expression. The evaluation of this expression determines the cost of the communication in terms of time, as function of system parameters. Many models have been proposed, covering different aspects of the communication. They can be generally classified in two types: *hardware models* and *software models*. Following, we introduce some of the representative models of each type.

Hardware models use hardware related parameters to build the analytical expression representing the cost of communications. LogP [10] is a foundational model representing the cost of a communication by four parameters: L is the *network delay*, and represent the latency of the network, o is the *overhead* or cycles that a CPU devotes to send the message, g is the *gap per message* and represents the minimum time interval between two consecutive injections to the network, and, finally, P is the number of processes. LogP model was improved by LogGP [27], which includes a new parameter G (gap per message) allowing to represent the influence of the network bandwidth in the transmission of large messages. In LogGP, the cost of a point-to-point transmission of a message of size m is represented as: $T_{p2p}(m) = 2o + L + (m-1)G$. More advanced models have been proposed, as PLogP [28], that considers parameters gap per message and overhead linear functions of the message size, achieving higher accuracy. Derived models have been proposed to represent communication costs in heterogeneous platforms, by extending previous purely homogeneous models with additional parameters representing specific features of the platform, as HLogGP [29] and LMO [30].

Software models address the modeling of the *middleware* costs of a communication. They abstract from hardware and use middleware-related parameters to build analytical expressions representing the costs associated to data movement. log_nP [31] considers a point-to-point transmission as a sequence of *transfers* (copies) through intermediate buffers between the endpoints of a homogeneous platform. The aggregation of the costs of the individual transfers yields the cost of the transmission in an expression as: $T(m) = \sum_{i=0}^{n-1} (o_i + l_i)$, where o (*overhead*) is the per transfer time dedicated by the CPU to a contiguous message, and the *latency* l is the additional cost if the message is non-contiguous in memory. τ-*Lop* model [32, 33] addresses the challenge of accurately modeling MPI communications on heterogeneous ultra scale platforms. It relies on the concept of *Concurrent Transfers* of data, and uses this concept as a building block to represent the communications on hierarchical communication channels, capturing the impact of contention and process mapping. The cost of a point-to-point message transmission is modeled using two parameters: the *overhead* $o^c(m)$ represents the time needed to start the injection of data in the communication channel c from the invocation of the operation, and the *transfer time* $L^c(m,\tau)$ is the time invested in each one of the data movements composing the transmission, and depends on the message size and the number of concurrent transfers progressing through the channel c. The parameter τ allows to the model to represent the cost derived from contention, and hence the channel bandwidth sharing, appearing naturally in collective and kernel communications. The τ-*Lop* expression describing the cost of a message transmission in n equal transfers is $T^c(m) = o^c(m) + n \times L^c(m,1)$. To represent the cost in complex heterogeneous platforms, τ-*Lop* adopts a compositional approach for representing the concurrency of full point-to-point transmissions, by using the concurrency operator $||$. As an example, the cost of the pair of concurrent transmissions is represented as $T^c(m) \mid\mid T^c(m) = 2 \mid\mid T^c(m) = o^c(m) + n \times L^c(m,2)$. Note how the amount of concurrent transmissions represented using the concurrency operator is propagated to the τ parameter of the transfers.

Using analytical models to optimize performance of complex heterogeneous kernels requires a high level of accuracy in the predictions and enough representation capabilities for the high amount of convoluted communications of the processes. Accuracy has to do with the representation of the cost, but also with the parameter measurement in the specific platform. A methodology for measuring the parameter values that captures the parameter meaning is essential for achieving accurate predictions of the communication cost.

Following, we develop an example of a simple communication optimization for a real data parallel kernel. The kernel (named *Wave2D*) uses the technique of finite differences to numerically solve the following wave equation in a $N \times N$ data space:

$$\frac{\partial^2 u}{\partial t^2} = c^2 \left(\frac{\partial^2 u}{\partial x^2} + \frac{\partial^2 u}{\partial y^2} \right) \tag{2.2}$$

Along time t, $u(x,y,t+1)$ is generated from its previous instances $u(x,y,t)$ and $u(x,y,t-1)$. The left side of Fig. 5 shows this matrix at a given step of the algorithm.

The communication optimization procedure departs from a previously established process distribution to the resources of the platform, involving multicore CPUs and accelerators. The first step is to balance the computational load between the processors. In a heterogeneous platform the processors have different computing capabilities, therefore, this step involves the characterization of the speeds of the processes by a vector $s = \{s_0, \ldots, s_{P-1}\}$, and the assignation to p_i of an amount of data proportional to its speed s_i. Usually, such speed characterization is done through benchmarking, that outputs a speed number per process, or a function describing the speed as a function of the task size (see section 2.1.2).

Regions of data distributed to the processes must tile the entire data space. Partitioning and distributing the data space in P regions of sizes proportional to s is subject to multiple variations, called *data mappings* . Alternatives data mappings can be evaluated to choose that which minimizes the communication cost. Note that, for the set of possible data mappings, every process performs the same amount of computational work on a different set of data points, and hence, the workload balance does not change, but does the communication cost. An example of a data mapping is shown at the right part of Figure 2.1. It represents the kernel running in an experimental platform composed of two nodes identified by a background color. The $P = 8$ processes communicate through shared memory or network depending on their location. Inside each node, each process may run on a set of assigned resources of different type. *FuPerMod* tool [34] was used to provide a load-balanced partition following a column-based approach [35]. Partitioning algorithms do not take into account the communication cost of the kernel, but only the relative speed of the processes. In this example, we use τ-*Lop* analytical framework to find a more efficient data mapping in terms of its communication costs.

In homogeneous systems, models of point-to-point and collective operations basically contains expressions in the forms $n \,||\, T^c(m)$ representing the cost of n concurrent transmissions of a message of size m through a communication channel c, and $T^c(m_1) \,||\, T^c(m_2)$, representing the cost of a sequence of two transmissions of different message sizes through the same communication channel. Communication models in heterogeneous systems become more complex. τ-*Lop* provides with extensions to evaluate these types of complex expressions [33] which shuffle concurrent and sequential transmissions of different message lengths progressing through the same or different communication channel, e.g. $T^{c_1}(m_1) \,||\, T^{c_2}(m_2)$. Anyway, expressions of actual kernels rapidly become complex enough to require an automatic evaluation. The τ-*Lop* toolbox[15] is a package that provides with a C++ function interface to describe and automatically evaluate the communication cost expressions of a data parallel kernel. Their inputs are the τ-*Lop* parameters built for the platform and a description of the data mapping and the kernel communications, both point-to-point and collectives. The toolbox provides with facilities to provide such description and to efficiently evaluate its communication cost. It allows to evaluate efficiently a set of partitions, leading to an optimal election.

[15]http://hpc.unex.es/taulop

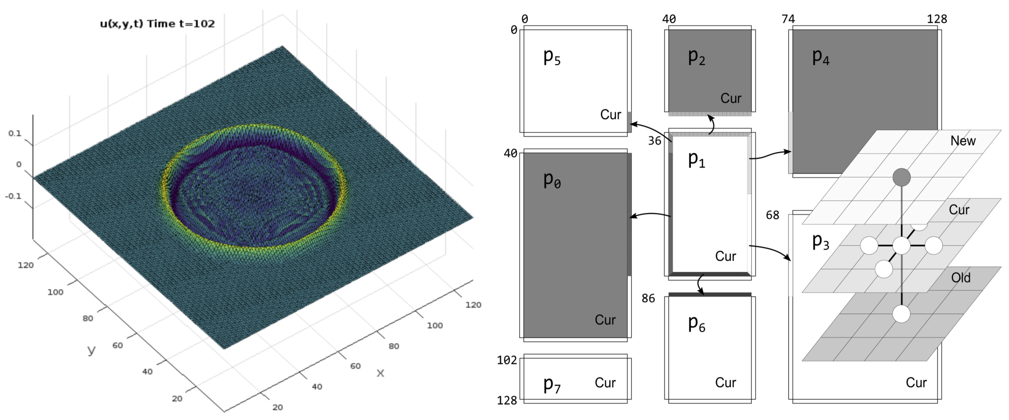

Figure 2.1: Left: visualization of discrete solution $u(x,y,t)$ of a wave equation in a $N \times N$ data mesh with $N = 128$, at time $t = 102$, for particular initial and boundary conditions. Right: an example data space partition and distribution to $P = 8$ processes with different computational capabilities running in two nodes (background color).

Algorithm 1 Code for evaluating the communication cost of the Wave2D kernel in a heterogeneous platform.

```
int P = 8;
int nodes = {0, 1, 0, 1, 0, 1, 1, 1}; // Node mapping
Process *p[P];
int *$\eta$[P];
for rank in {0, P-1}:
p[rank] = new Process (rank, nodes[rank]);
for rank in {0, P-1}:
$\eta$[rank] = new Neighbors (p);
TauLopConcurrent *conc = new TauLopConcurrent ();
for rank in {0, P-1}:
TauLopSequence *seq = new TauLopSequence ();
for dst in {$\eta$[rank]}:
m = getMsgSize (p, dst) * sizeof(double);
seq$\rightarrow$add (new Transmission (p[rank], p[dst], m));
conc$\rightarrow$add(seq);
TauLopCost *tc = new TauLopCost ();
conc$\rightarrow$evaluate (tc);
double t = tc$\rightarrow$getTime ();
```

As shown in the right part of Figure 2.1, at each time $t+1$, every data point in matrix *New* is calculated as a combination of the neighbor points in matrix *Cur*, which requires a previous communication stage of the needed data from neighbor processes at step t. Such communications are represented in the figure for process p_1. As the computation is (unevenly) load balanced, all processes come into the communication phase at the same time. Hence, all processes interchange their boundaries simultaneously. From this assumption, we can derive a communication cost expression of the kernel:

$$\Theta = t \times \left[\overset{P-1}{\underset{p=0}{||}} \Theta_p \right], \; with\, \Theta_p = \sum_{i \in \eta_p} T^{c(i)}(m(i)). \tag{2.3}$$

All of the processes communicate concurrently, so the total cost Θ is calculated using the concurrency operator $||$ for every process communication over t steps. A process p transmits its boundary data to its neighbor processes (the set η_p) using the channel $c(i)$ for transmitting the message of size $m(i)$ to the neighbor i. The transmissions of a process to its neighbors are accomplished sequentially, hence the sum.

Extending previous cost expression to every individual cost transmission is indeed complex enough to require evaluation using an automatic tool. Code 1 uses τ-*Lop* toolbox to describe and evaluate the previous cost model representing the communications and data mapping of the kernel. Array `node` represents the mapping of processes to nodes, numbered 0 and 1. Following, an array of processes is created, with the rank number and mapping node of each `Process`. Then, `Neighbors()` function is used to create the neighbor set of each process (η_p). Neighbor sets are specific for a given arrangement of the rectangles in the data space (data mapping) and determine the destination and amount of data transmitted through different communication channels, and, as a consequence, the final cost. As an example, Figure 2.2 shows two partitions with different communication costs. At the left figure the number of data points in process p_5 boundaries for transmitting through the network to processes in $\eta_5 = \{0,1,2\}$ is 76, while at the right figure, with $\eta'_5 = \{0,3,7\}$, the number is 40, reducing the transmissions through the slower network communication channel, and hence, the cost. The rest of the code composes and evaluates the cost for the specific partition. The cost expression is composed using the `TauLopConcurrent` and `TauLopSequence` objects. All Transmissions added to a `TauLopSequence` object will be evaluated under the assumption that they progress sequentially. Then, `TauLopSequence` objects added to a `TauLopConcurrent` object will be evaluated under the assumption that they progress concurrently, applying the transfer time parameter values for specific m and τ. The communication channel used for each transmission is internally figured out from the node location obtained from the processes. Finally, `TauLopCost` object evaluates the cost expression and returns a time in seconds.

By executing the algorithm using all possible data mappings, the optimum arrangement is obtained. Actually, this procedure is unfeasible when the number of processes grows, because the number of combinations grows exponentially. In practice, only a reduced set of possible data mappings is evaluated. A straightforward heuristic-based optimization decision for Wave2D, proposed by Malik et al [36], is based on the rearrangement of the regions assigned to processes running on the same node to be as close as possible, which decreases the network communication, more expensive in terms of time.

2.1.4 Power and Energy Models of Computation

In this section, we will survey research works that have proposed power and energy predictive models for optimization of applications for energy on ultrascale systems.

There are several ways to classify power and energy predictive models for ultrascale computing systems and applications.

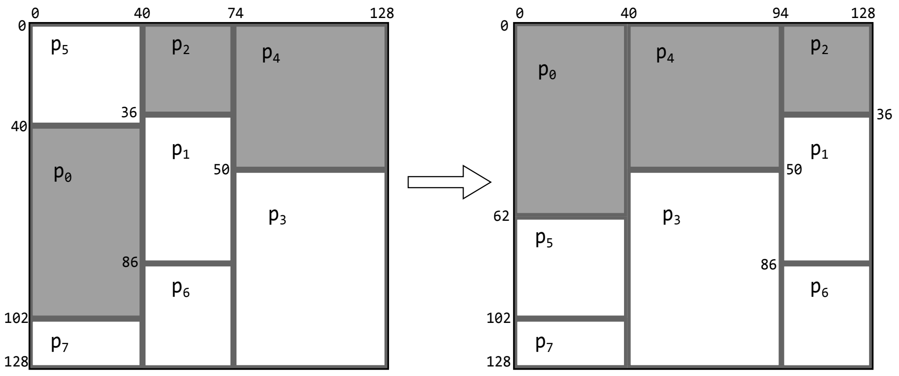

Figure 2.2: Rearranging the data regions assigned to processes in the 2D mesh data space in such a way that network transmissions have been minimized.

First classification is based on three dominant approaches used for modeling power and energy consumption.

- ***System-level***: The approach is to use system-level physical measurements using power meters.
- ***On-chip sensors***: On-chip sensors supplied by the vendors and their APIs are used for obtaining the power and energy consumptions.
- ***Performance Monitoring Events (PMCs)***: This dominant approach uses the PMCs provided by a vendor as parameters for the models.

Second classification is based on the characteristic *Level of abstraction*, which specifies how the model captures the inherent hierarchical and heterogeneous nature of modern processor architectures.

- ***Linear Independence*** - All the components of a node are modeled independently. The model for a node is a linear combination of the models of its components.
- ***Linear Dependence*** - The components of a node are modeled taking into account the dependencies (shared structures) between them and expressing these dependencies linearly. For example:
  - The models for CPUs are constructed taking into account the shared resources (Last level cache) between them.
  - For an application employing both CPUs and accelerators, the models for CPUs and the accelerators are constructed taking into account the shared resources (last level cache) between the CPUs and the communication link (PCIe) connecting the CPUs and the accelerators.
- ***Non-linear Independence*** - All the components of a node are modeled independently. However, the model for a node is a non-linear combination of the models of its components.
- ***Non-linear Dependence*** - This is the most complex model. The components and dependencies between them (shared resources, communication links) are modeled non-linearly by taking into account their inherent hierarchical and heterogeneous nature.

From our survey, almost all the models fall into the category of *linear independence*.

However, we divide our survey into categories using the following more readable classification: a). Models for CPUs, b). Models for GPUs, c). Models for Xeon Phis and FPGAs, d). Application-specific models, and e). Critiques of PMC-based models.

Owing to length constraints, we will look at only the most prominent works in each category.

Power and Energy Models for CPUs. The first notable model in this category is [37], which is based on events such as integer operations, floating-point operations, memory requests due to cache misses, etc. that the authors believed to strongly correlate with power consumption. Icsi et al. [38] propose a methodology to determine unit-level power estimates based on hardware performance counters. They select 22 strictly collocated physical units based on an annotated P4 die photo. The total power consumption is then estimated as the sum of the power consumptions of the

22 physical units plus the base power. The power estimate for each unit is a linear function of the access rate of it, with the exception of few issue logic units where an extra parameter is introduced to model the non-linear behavior.

Several models employed as predictor variables utilization metrics of the key components such as CPU, memory, disk, and network. The most comprehensive model in this group is proposed in [39] that used as parameters, the utilization metrics of CPU, disk, and network components and hardware performance counters for memory. Here, the general model can be described as follows:

$$P = C_{base} + C_1 \times U_{CPU} + C_2 \times U_{Mem} + C_3 \times U_{Disk} + C_4 \times U_{Net} \tag{2.4}$$

where C_{base} is the base power consumption of a node and U_{CPU}, U_{Mem}, U_{Disk}, and U_{Net} are the CPU, memory, disk, and network utilizations respectively.

Basmadjian et al. [40] construct a power model of a server as a summation of power models of its components, the processor (CPU), memory (RAM), fans, and disk (HDD). Bircher et al. [41] propose a non-linear model to predict power using PMCs. They use PMCs that trickle down from the processor to other subsystems such as CPU, disk, GPU, etc and PMCs that flow inward into the processor such as Direct Memory Access (DMA) and I/O interrupts.

Power and Energy Models for GPUs. GPUs are now an integral part of high performance computing systems due to their enormous computational powers and energy efficiency (performance/watt). In a node, the GPU is used as a coprocessor and is connected to a CPU through a PCI-Express (PCIe) bus. Work is offloaded from a CPU to the GPU.

The first comprehensive model developed for GPUs was by [42]. The GPU power consumption in their prediction model is modelled similar to the PMC-based unit power prediction approach of [38]. In their model, the power consumption is calculated as sum of power consumptions of all the components composing the Streaming Multiprocessor (SM) and GDDR memory.

Majority of other models employ machine learning methods. [43] propose power and energy prediction models that employ a configurable, back-propagation, artificial neural network (BP-ANN). The parameters of the BP-ANN model are ten carefully selected PMCs of a GPU. The values of these PMCs are obtained using the CUDA Profiling Tools Interface (CUPTI) [44] during the application execution. [45] use the technique of program slicing to model GPU power consumption. The source code of an application is decomposed into slices and these slices are used as basic units to train a power model based on fuzzy wavelet artificial neural networks (FWNN). So, unlike earlier research efforts which use PMCs, slicing features are extracted from the programs and used in their model.

Power and Energy Models for Xeon Phis and FPGAs. In this category, we cover the other accelerators that are used in high performance computing systems.

There is an abysmal shortage of power and energy prediction models for Xeon Phis. We found just one for Xeon Phis even though this accelerator enjoys a noticeable space in the Top500 [46] supercomputers. [47] construct an instruction-level energy model of a Xeon Phi processor and report an accuracy between 1% and 5% for real world applications.

To the best of our knowledge, there are no linear regression models using PMCs because PMCs are not yet offered by FPGAs. [48] construct a linear energy prediction model based on instruction level energy profiling. [49] propose a linear component-based model to predict energy consumption of a reconfigurable Multiprocessors-on-a-Programmable-Chip (MPoPCs) implemented on Xilinx FPGAs. [50] propose a linear instruction-level model to predict dynamic energy consumption for soft processors in FPGA. The model considers both inter-instruction effects and the operand values of the instructions.

Application-specific Models. Here, we present studies for saving power and energy in HPC applications. Previous sections dwelt on power and energy models for dominant components in a node that predicted power and energy consumptions for all kinds of applications executing on these components. Our focus in this category is application-specific.

Lively et al. [51] propose application-centric predictive models for power consumption. For each kernel in an application, multivariate linear regression models for system power, CPU power, and memory power are constructed using PAPI performance events [52] as predictors.

[53] compare the power consumptions of two high performance dense linear algebra libraries i.e., LAPACK and PLASMA. Their results show that PLASMA outperforms LAPACK both in performance as well as energy efficiency.

[54], [55] propose system-wide power prediction models for HPC servers based on performance counters. They cluster real-life HPC applications into groups and create specialized power models for them. They then use decision trees to select an appropriate model for the current system load.

Lastovetsky et al. [56] present an application-level energy model where the dynamic energy consumption of a processor is represented by a function of problem size. Unlike PMC-based models that contain hardware-related PMCs and do not consider problem size as a parameter, this model takes into account highly non-linear and non-convex nature of the relationship between energy consumption and problem size for solving optimization problems of data-parallel applications on homogeneous multicore clusters for energy.

Critiques of PMC-based models. In this category, we review attempts that have critically examined and highlighted the poor prediction accuracy of PMCs for energy predictive modeling.

Economou et al. [39] highlight the fundamental limitation, which is the inability to obtain all the PMCs simultaneously or in one application run. They also mention the lack of PMCs to model energy consumption of disk I/O and network I/O. McCullough et al. [57] evaluate the competence of predictive power models for modern node architectures and show that linear regression models show prediction errors as high as 150%. They suggest that direct physical measurement of power consumption should be the preferred approach to tackle the inherent complexities posed by modern node architectures. Hackenberg et al. [58] present a study of various power measurement strategies, which includes *Intel RAPL* [59]. They report that the accuracy of *RAPL* depends on the type of workload and is quite poor for workloads that use the hyper-threading feature. They also report that the accuracy is poor for applications with small execution times and becomes better only for applications with longer execution times since the predictions are energy averages.

O'Brien et al. [60] survey predictive power and energy models focusing on the highly heterogeneous and hierarchical node architecture in modern HPC computing platforms. Using a case study of PMCs, they highlight the poor prediction accuracy and ineffectiveness of models to accurately predict the dynamic power consumption of modern nodes due to the inherent complexities (contention for shared resources such as Last Level Cache (LLC), NUMA, and dynamic power management). Arsalan et al. [61] propose a novel selection criterion for PMCs called *additivity*, which can be used to determine the subset of PMCs that can potentially be considered for reliable energy predictive modelling. They study the *additivity* of PMCs offered by two popular tools, *Likwid* [62] and *PAPI* [52], using a detailed statistical experimental methodology on a modern Intel Haswell multicore server CPU. They show that many PMCs in *Likwid* and *PAPI* are *non-additive* and that some of these PMCs are key predictor variables in energy predictive models thereby bringing into question the reliability and reported prediction accuracy of these models.

Prominent Surveys on Power and Energy Predictive Models.

In this category, we present recent surveys summarizing the power and energy efficiency techniques employed in high performance computing systems and applications.

Mobius et al. [63] present a survey of power consumption models for single-core and multicore processors, virtual machines, and servers. They conclude that regression-based approaches dominate and that one prominent shortcoming of the these models is that they use static instead of variable workloads for training the models.

Inacio et al. [64] present a literature survey of works using workload characterization for performance and energy efficiency improvement in HPC, cloud, and big data environments. They report a remarkable increase in research papers proposing energy modelling and energy efficiency techniques from 2009 to 2013 thereby suggesting an increasing importance of energy saving techniques in the HPC, cloud, and big data environments.

Tan et al. [65] survey the research on saving power and energy for HPC linear algebra applications. They separate the surveyed efforts into two categories: 1) Power management in HPC systems and 2) Power and energy efficient HPC applications (Cholesky, LU, QR). They construct a linear model of a HPC system as a summation of power consumptions of all the nodes in the system. The power consumption of a node is modelled as the sum of all the major components (CPU, GPU, RAM) of a node.

Dayarathna et al. [66] present an in-depth and voluminous survey on data center power modelling.

O'Brien et al. [60] survey the state-of-the-art energy predictive models in HPC and present a case study demonstrating the ineffectiveness of the dominant PMC-based modeling approach for accurate energy predictions.

2.1.5 Holistic Approaches to Optimization for Performance and Energy

In this section, we will review research that has proposed solutions for optimization of scientific applications on ultrascale platforms for both performance and energy. We believe that realistic and accurate performance and energy models of computations and communications are fundamental to the effectiveness of these solution approaches.

The methods solving the bi-objective optimization problem for performance and energy (*BOPPE*) can be broadly classified as follows:

- *System-level*: Methods that aim to optimize several objectives of the system or the environment (for example: clouds, data centers, etc) where the applications are executed. The leading objectives are performance, energy consumption, cost, and reliability. A core characteristic of the methods is the use of application-agnostic models for predicting the performance of applications and energy consumption of resources in the system.
- *Application-level*: Methods focusing mainly on optimization of applications for performance and energy. These methods use application-level models for predicting the performance and energy consumption of applications. This category can be further sub-classified into methods that target intra-node optimization and methods that target both intra-node and inter-node optimization.

System-level: Mezmaz et al. [67] propose a parallel bi-objective genetic algorithm to maximize the performance and minimize the energy consumption in cloud computing infrastructures. Fard et al. [68] present a four-objective case study comprising performance, economic cost, energy consumption, and reliability for optimization of scientific workflows in heterogeneous computing environments. Beloglazov et al. [69] propose heuristics that consider twin objectives of energy efficiency and Quality of Service (QoS) for provisioning data center resources. Kessaci et al. [70] present a multi-objective genetic algorithm that minimizes the energy consumption, CO2 emissions, and maximizes the generated profit of a cloud computing infrastructure. Durillo et al. [71] propose a multi-objective workflow scheduling algorithm that maximizes performance and minimizes energy consumption of applications executing in heterogeneous high-performance parallel and distributed computing systems.

Application-level: Freeh et al. [72] propose an intra-node optimization approach that analyzes the performance-energy trade-offs of serial and parallel applications on a cluster of DVFS-capable AMD nodes. In their study, they consider three intra-node parameters to characterize the performance and energy of serial and parallel applications. Ishfaq et al. [73] formulate a bi-objective optimization problem for power-aware scheduling of tasks onto heterogeneous and homogeneous multicore processor architectures. Their solution method targets intra-node optimization. They consider intra-node parameters such as DVFS, computational cycles, and core architecture type. Balaprakash et al. [74] is an intra-node optimization approach that explores trade-offs among power, energy, and performance using various application-level tuning parameters such as number of threads and hardware parameters such as DVFS.

Drozdowski et al. [75] propose a concept called an iso-energy map, which represents points of equal energy consumption in a multi-dimensional space of system and application parameters. They study three analytical models, two intra-node and one inter-node. For the inter-node model, they consider eight parameters. From all the possible combinations of these parameters, they study twenty-eight combinations and their corresponding iso-energy maps. However, one of the key assumptions in their model is that the energy consumption is constant and independent of problem size. Marszakowski et al. [76] analyze the impact of memory hierarchies on performance-energy trade-off in parallel computations. They study the effects of twelve intra-node and inter-node parameters on performance and energy. In their problem formulations, they represent performance and energy by two linear functions of problem size, one for in-core computations and the other for out-of-core computations.

Reddy et. al. [77] study the bi-objective optimization problem for performance and energy (*BOPPE*) for data-parallel applications on homogeneous clusters of modern multicore CPUs, which is based on only one but heretofore unstudied decision variable, the problem size. They present an efficient and exact global optimization algorithm that solved the *BOPPE*. It takes as inputs, functions of performance and dynamic energy consumption against problem size, and outputs the globally Pareto-optimal set of solutions. These solutions are the workload distributions, which achieve inter-node optimization of data-parallel applications for performance and energy.

2.2 Impact of Workflow Enactment Modes on Scheduling and Workflow Performance

In the past decade, computer architectures have experienced an important paradigm shift. From a single processor containing a few homogeneous cores, computers have evolved to complex dynamic systems containing tens or hundreds of heterogeneous computing resources, the so-called *manycore* computers. Despite these trends, the majority of popular parallel programming languages, development tools and compilers remain to be based on the old symmetric multi-processing paradigm. Past efforts to make parallel computers more accessible for programmers resulted in a multitude of different and often incompatible programming libraries and language extensions, including successful standards like OpenMP, OpenCL and MPI.

On distributed computing infrastructures (DCIs), *scientific workflows* emerged in industry, business and science as an easy way to develop large-scale applications as a composition of smaller loosely-coupled components [78]. Existing DCI workflow engines are currently mature and come with rich ecosystems which support the user in all aspects of a workflow lifecycle from creating to execution, monitoring and results retrieval, interfaced towards the domain scientists and ease of use rather than the computer science underneath [79, 80, 81, 82, 83, 84]. Because of the similarity in terms of scale and heterogeneity, workflow systems represent today a promising alternative for development and execution of scientific applications on shared memory heterogeneous manycore architectures. However, existing workflow engines targeted at DCIs are prone to high overheads and latencies [1]. While such overheads are acceptable on DCIs, tightly-coupled manycore computers are much more sensitive to latencies and other form of overheads.

To overcome these problems, Janetschek *et al.* [1] presented a *Manycore Workflow Runtime Engine (MWRE)* that efficiently exploits the low latency characteristics of heterogeneous manycore computers and which performs significantly better than traditional workflow engines on manycore computers.

There are two different strategies for enacting a workflow determining how and when the workflow engine evaluates a workflow execution plan: *early* and *late evaluation mode*. In theory, early enactment mode produces a better workflow schedule, while also having more enactment overhead. Late enactment mode theoretically produces a worse workflow schedule, while having less enactment overhead. The practical implications of early and late enactment modes on scheduling performance are still unclear, therefore, in this work we simulated the execution of a large number and variety of random MWRE workflows with both early and late evaluation mode to gain more insights on how much early evaluation mode improves scheduling performance and to be able to deduct some guidelines on when to use early evaluation mode and when to use late evaluation mode.

Next, the following topics are addressed. Section 2.2.1 introduces the scientific workflow model, followed by an introduction to workflow enactment in Section 2.2.2 and to workflow scheduling in Section 2.2.3. Section 2.2.4 explains the MWRE workflow engine for manycores. Section 2.2.5 discusses the theoretical implications of an incomplete workflow execution plan on scheduling, followed by an explanation of the methodology used to conduct the experiments presented in Section 2.2.6. Section 2.2.7 discusses experimental results, and Section 5.3.5 presents conclusions.

2.2.1 Scientific Workflow Model

A workflow consists of two parts: an *abstract* part and a *concrete* part. A short overview of these two parts is presented next.

Workflow Abstract Part

The abstract part (see Figure 2.3) of a scientific workflow comprises a hardware and middleware agnostic (and therefore portable) description of its structure, the activities involved (identified by a unique name and a type), and the data and control-flow dependencies between the activities. The individual activities are treated as black-boxes where only the input and output signatures are known.

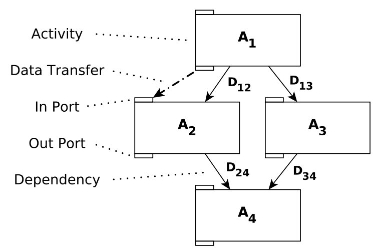

Figure 2.3: Abstract part of a scientific workflow.

There are usually two different types of workflow activities:

1. *Atomic activities* are basic indivisible units of computation;

2. *Composite activities* combine several fine granular activities, including atomic and other composite activities, to form coarse grained activities and impose a control flow on the contained inner activities.

Typical composite activities are sequential and parallel loops, conditional activities and sub-workflows.

Workflow Concrete Part

The concrete part of a workflow contains the hardware and middleware-dependent implementations of the atomic activities and their accompanying meta-information. This part is often highly specific to each individual workflow system and the underlying computing infrastructure. It usually contains information about the available activity implementations, locations where they are installed, how they can be executed, and any other further information intended to help the workflow engine in selecting the most appropriate activity implementation.

2.2.2 Workflow Enactment

A workflow engine executes a workflow instance (operation usually called *workflow enactment*) by traversing the DAG representing the workflow structure, determining the state of the individual activities, transferring data from finished activities to their successors in the dependency graph, unrolling composite activities and replacing them with the resulting subgraph, and delegating the actual execution of atomic activities to the scheduling and execution subsystems. We call the resulting DAG, where composite activities have been replaced with their contained subgraphs and enriched with additional state information, a *workflow execution plan (WEP)* .

We distinguish between two types of workflow enactment modes [1]:

1. *Early enactment mode*, where the engine reevaluates the WEP as soon as there are activity state changes, and completes it as early as possible. This mode usually comes with a much higher overhead, but results in a more complete WEP comprising more information, which allows the scheduler to better plan the workflow execution on the underlying resources;
2. *Late enactment mode* (also called lazy evaluation mode), where the engine only partially reevaluates and completes the WEP when it is absolutely necessary for further workflow enactment. This mode has less overhead, but also results in a less complete WEP with less information available for the scheduler to plan the workflow execution.

2.2.3 Workflow Scheduling

Workflow scheduling describes the process of mapping atomic activities to available computing resources where they are executed. The resulting mapping of activities to computing resources is called *workflow schedule*. The scheduler optimizes the workflow schedule by maximizing or minimizing a given utility function, typically the overall execution time. Some scheduler implementations take more than one objective into account, some of which being in conflict with each other and requiring *multi-objective optimization* [85], or by considering one variable as a constraint [86] while optimizing the other.

Generating a full-ahead schedule is an NP-hard problem [87] and therefore, most existing full-ahead scheduling methods are approximate heuristic algorithms [88]. Existing scheduling heuristics can be broadly divided into the two following categories [89]:

1. *Just-in-time scheduling algorithms*: only consider the next activities to be scheduled when deciding on a mapping and ignore the rest of the WEP. They are usually linear in complexity with the number of activities (i.e. $O(N)$) and have a low overhead, but as a consequence produce poorer schedules;
2. *Full-ahead scheduling algorithms*: use the entire WEP when deciding on a mapping. They usually present a higher overhead, but consider more workflow information and therefore, produce in general better results.

2.2.4 Manycore Workflow Runtime Engine

We designed and developed a workflow engine called *Manycore Workflow Runtime Engine* (MWRE) [1], specifically tuned for shared-memory heterogeneous manycore parallel computers. Our motivation is to exploit the workflow paradigm, highly successful for programming DCIs (like Clouds), for programming heterogeneous manycore architectures, while supporting and integrating existing established parallel programming paradigms, such as OpenMP. Traditional workflow applications in DCIs usually have a rather simple structure, feature a coarse-grained parallelism with relatively few long-running parallel tasks, and exhibit large task submission and data transfer overheads. In contrast, shared memory manycore applications usually have a much more complex structure, feature a more fine-grained parallelism with a lot of short running parallel tasks, and hardly have any task submission and data transfer overheads.

The defining feature of our engine is compiling workflows into semantically-equivalent C++ programs using a source-to-source compiler (and not interpreting workflows like most traditional engines for DCIs). The workflow engine is linked to the C++ program in the form of a shared library that uses a novel callback-driven enactment mechanism, where the engine is only responsible for maintaining and traversing the WEP. Dependency resolution and data transfers are implemented in callback functions, specifically tailored to the concrete workflow and are part of the workflow specification. This keeps the engine clean and minimizes the enactment overhead.

2.2.5 Impact of Incomplete WEP on Full-Ahead Scheduling

When using a full-ahead scheduling algorithm, the workflow enactment mode can theoretically have a huge influence on the scheduling performance. Full-ahead

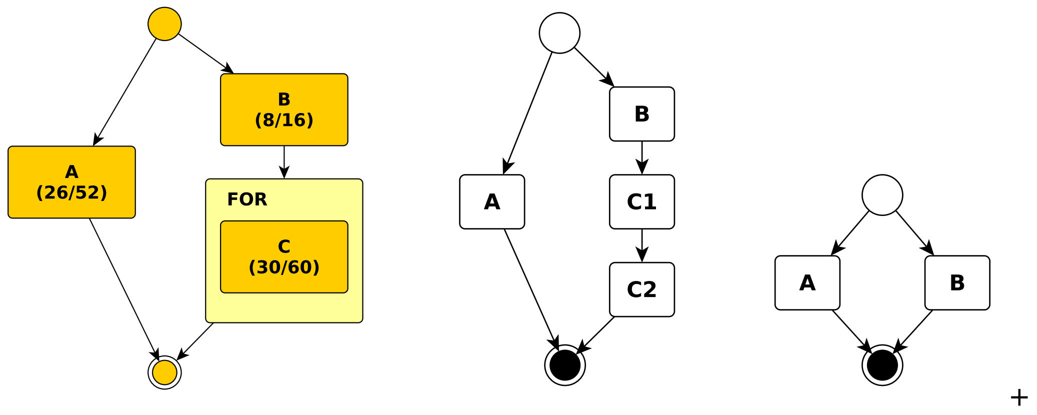

(a) Example workflow. (b) Early enactment mode. (c) Late enactment mode.

Figure 2.4: WEPs in early and late enactment mode at workflow execution start for an example workflow, where the numbers in brackets represent the execution times on resources $R1$ and $R2$.

scheduling considers the entire WEP when calculating a schedule, therefore an incomplete WEP may lead to a comparatively worse workflow schedule.

For example, let us assume the workflow in Figure 2.4a executed on a heterogeneous system consisting of two different computing resources: resource $R1$ and resource $R2$. Resource $R1$ has a fast CPU, and resource $R2$ has a twice as slow CPU. The example workflow consists of two parallel atomic activities A and B, and a sequential `for` loop with a data dependency on activity B containing a single atomic activity C. The number of iterations of the `for` loop is known from the beginning and assumed here as two. The number in brackets represents the activity execution times on resources $R1$ and $R2$, respectively.

Most full-ahead scheduling algorithms try to prioritize the atomic activities lying on the workflow's *critical path*, defined as the longest path from the start to the end of the workflow, and the *length* of the critical path is defined as the sum of the activity execution times on the critical path. The activities on the critical path have the most influence on performance, and any delay on the critical path delays the entire workflow.

The critical path of our example workflow consists of activities B, $C1$ and $C2$ (where $C1$ refers to the instance of C in the first loop iteration, and $C2$ to the instance of C in the second loop iteration), and the minimum length of the critical path is 68. Therefore, an optimal workflow schedule maps activity A to resource $R2$, and activities B, $C1$ and $C2$ to resource $R1$ to achieve a workflow makespan of 68.

When using early enactment mode the `for` loop is immediately evaluated and the resulting WEP (see Figure 2.4b) contains all the necessary information to find the correct critical path. Therefore a full-ahead scheduling algorithm can calculate an optimal workflow schedule as depicted above.

In late enactment mode, the evaluation of the `for` loop is deferred until activity B has finished its execution. Therefore, the resulting WEP (see Figure 2.4c) initially

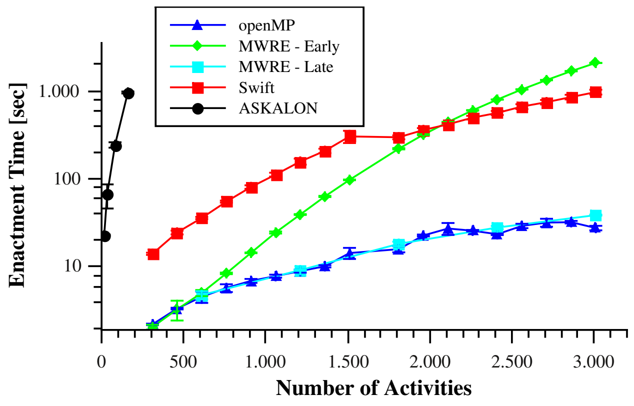

Figure 2.5: Enactment times of the Montage workflow [1].

misses the activities $C1$ and $C2$, and a full-ahead scheduler would base it's calculation of a workflow schedule on incomplete information. It may be deducted from the WEP that the critical path only consists of activity A and map it onto the fastest resource $R1$, while activity B is mapped onto the slower resource $R2$. The `for` loop will be evaluated only after activity B has finished and the WEP will look like Figure 2.4b. At this time, the critical path activity B has already been executed by the slower resource, and resource $R1$ is still occupied executing activity A. Therefore, the scheduler can only map activity $C1$ onto the slower resource, $C2$ is the only critical path activity mapped to the fastest resource. The workflow makespan in this scenario is 106, which is about 56% larger than the optimal makespan.

Based on this observations, one may conclude that early enactment mode should always be preferred to late enactment mode. However, our experience with MWRE has shown that depending on the particular workflow to be executed, early enactment mode can exhibit drastic performance losses and a limited scalability compared to late enactment mode. For example, Figure 2.5 (taken from [1]) shows the enactment overhead of the Montage workflow executed with MWRE, referring to the time spend in the engine not including the execution times of the atomic activities. In this experiment we executed the Montage workflow several times with a different number of atomic activities. The enactment time in late enactment mode stays close to the enactment time of an equivalent OpenMP program for the whole experiment. In contrast, the enactment time of early enactment mode is also close to the enactment time of the OpenMP version in the beginning, but significantly increases beyond 600 activities.

2.2.6 Methodology

To evaluate the impact of early and late evaluation mode on scheduling performance, we simulated the execution of a large number and variety of workflows on manycore architectures. Due to the lack of a sufficient number of complex real-world workflows, we used an algorithm to generate a large number of random workflows with varying parameters.

Algorithm 2 Random hierarchical workflow generation.

```
1: procedure GENRANDOMWORKFLOW($v, \alpha, o, w, \beta, l$)
2:     $W \leftarrow$ ORIGGENRANDOMWORKFLOW($v, \alpha, o, w, \beta$)
3:     if $l > 1$ then
4:         $s \leftarrow$ SELECTRANDOMACTIVITY($W$)
5:         $t \leftarrow$ SELECTRANDOMCOMPOSITETYPE(if,parallel for)
6:         $SW[0] \leftarrow$ GENRANDOMWORKFLOW($v, \alpha, o, w, \beta, l-1$)
7:         if $t =$ if then
8:             $SW[1] \leftarrow$ GENRANDOMWORKFLOW($v, \alpha, o, w, \beta, l-1$)
9:         end if
10:        CONVERTATOMICTOCOMPOSITE(s, t, SW)
11:        $p \leftarrow$ SELECTRANDOMPREDECESSOR($s$)
12:        $h \leftarrow$ CREATEHELPERNODE($t$)
13:        INSERTNODE($h, p, s$)
14:    end if
15:    return $W$
16: end procedure
```

Random Workflow Generation

For generating random workflows, we used an existing algorithm [88] that creates workflows consisting of solely atomic activities, extended to cover composite ones, as shown in Algorithm 2. The algorithm considers the following parameters as input to influence the shape and structure of the generated workflows:

- *Average number of activities v* in the workflow;
- *Workflow shape* α by randomly generating the workflow height from a uniform distribution with a mean value of $\frac{\sqrt{v}}{\alpha}$ and the width of each level from a uniform distribution with a mean value of $\sqrt{v} \cdot \alpha$;
- *Output degree o* of an activity, which is the maximum number of successors a workflow activity is allowed to have;
- *Average execution time w* of an atomic activity;
- *Computational heterogeneity* β by randomly selecting the execution time of an activity on a specific resource from the interval $\left(w \cdot \left(1 - \frac{\beta}{2}\right), w \cdot \left(1 + \frac{\beta}{2}\right)\right)$;
- *Maximum nesting level l* of the composite activity.

At first, a workflow is generated using the original algorithm (line 2). As long as the maximum nesting level has not been reached, a random activity is selected (line 4), a random composite activity type is chosen (line 5), one or two sub-workflows representing the body of the composite activity are created by recursively calling the algorithm (lines 6 –9), and finally the selected activity is converted into the corresponding composite activity (line 10). Next we select a random predecessor (line 11) of the composite activity, which supplies it with specific input data, such as conditional argument for `if` activities and loop counter boundaries for *parallel for* activities. To ease implementation of the algorithm composite activity specific

Parameter	*Symbol*	*Value set*
Average number of activities	v	10
Workflow shape	α	$\{0.1, 0.5, 1.0, 1.5, 2.0\}$
Activity output degree	o	$\{1, 3, 20\}$
Activity average execution time	w	3 seconds
Computational heterogeneity	β	3.0
Maximum nesting level	l	$\{1, 2\}$

Table 2.1 Random workflow generation parameters.

Configuration	*Description*
Configuration 1	4 different single-core CPUs
Configuration 2	8 different 10-core CPUs
Configuration 3	1 4-core CPU and 2 different GPUs

Table 2.2 Simulated hardware configurations.

data is supplied by a helper activity inserted between the selected predecessor and the composite activity (lines 12 and 13). The helper activity randomly chooses for `if` activities whether the supplied condition is `true` or `false`, and the loop iteration count between 2 and 10 for `parallel for` activities.

Experimental Setup

We conducted our experiments by generating five different workflows for each parameter combination (see Table 2.1), and then simulated the execution of each workflow five times for both evaluation modes on three heterogeneous hardware configurations (see Table 2.2) using seven different schedulers.

The workflow generation parameters were chosen to best represent the characteristics of manycore workflow applications, characterized by a relatively high number of short running activities. The generated workflows consist of $20 - 110$ unique activities, each having a different randomly chosen execution time of 0.1 to 6 seconds for each resource type. The workflows have highly different shapes, ranging from nearly sequential to workflows with a high degree of parallelism, and from workflows with very few dependencies between activities to nearly fully connected ones. Larger workflows were not created, as MWRE early evaluation mode leads from our experience to a significant increase in enactment overhead (e.g. see Figure 2.5) beyond a few hundred workflow activities. For the experiments, we aimed to have early and late evaluation modes with roughly the same enactment overhead to not bias the results.

To get meaningful results independent from a specific scheduler, the following schedulers implemented in MWRE were used:

- *Minimum Completion Time* (MCT) [90] is a just-in-time algorithm that assigns ready-to-execute tasks in no particular order to the resource with the minimum completion time.
- *Heterogeneous Earliest Finish Time* (HEFT) [88] is a list based heuristic consisting of two phases. In the ranking phase all tasks are assigned a rank representing the longest path from the task to the exit node. In the processor selection phase the tasks are assigned to a free processor with the earliest finish time in the order of their ranks.
- *Predict Earliest Finish Time* (PEFT) [91] is also a list based heuristic similar to HEFT, which uses the average path from the task to the exit node for assigning a rank.
- The *Lookahead* [92] algorithm is another variant of HEFT also taking the children of a task into account in the processor selection phase.
- The *Min-Min* [90] is a batch mode heuristic consisting of two phases. In the first phase the minimum expected completion time is calculated for each task, and in the second phase the tasks are assigned to processors according to their minimum expected completion time in the order of the overall minimum expected completion time.
- The *Max-Min* [90] scheduling algorithm is very similar to Min-Min except that the second phase takes the maximum expected completion time into account.
- The *Sufferage* [90] scheduling algorithm assigns tasks to processors according to how much the task would "suffer" in terms of expected completion time if it is not assigned to that processor.

For each workflow the average makespan, hardware configuration, scheduler and evaluation mode combination are registered. The results are grouped according to the scheduler, hardware configuration, workflow shape, activity output degree and composite activity nesting level, and the relative time difference $\Delta T_{rel} = \frac{T_{late} - T_{early}}{T_{late}}$ of the makespan of early evaluation mode T_{early} compared to the makespan of late evaluation mode T_{late} is calculated. If the relative time difference is less than $\pm 2.5\%$, it is assumed there is no significant difference. It is determined the relative number of experiments showing no significant performance improvement, the relative number of experiments showing a significant performance improvement with early evaluation mode, and the relative number of experiments showing a significant performance degradation.

Simulations are run on an Intel Core i7-2600K running at 3.40GHz with 16GB RAM.

2.2.7 Experimental Results

The results of all experiments are shown in Figure 2.6. For 85.7% of the experiments, the workflow makespan in early evaluation mode is nearly the same as the makespan in late evaluation mode. For 11.6% of all experiments the early evaluation mode is faster, while for 2.7% it is slower than late evaluation mode. In the best case early evaluation mode is 43% faster, and in the worst case early evaluation mode is 39.6% slower. The experiments for which early evaluation mode is faster show an average

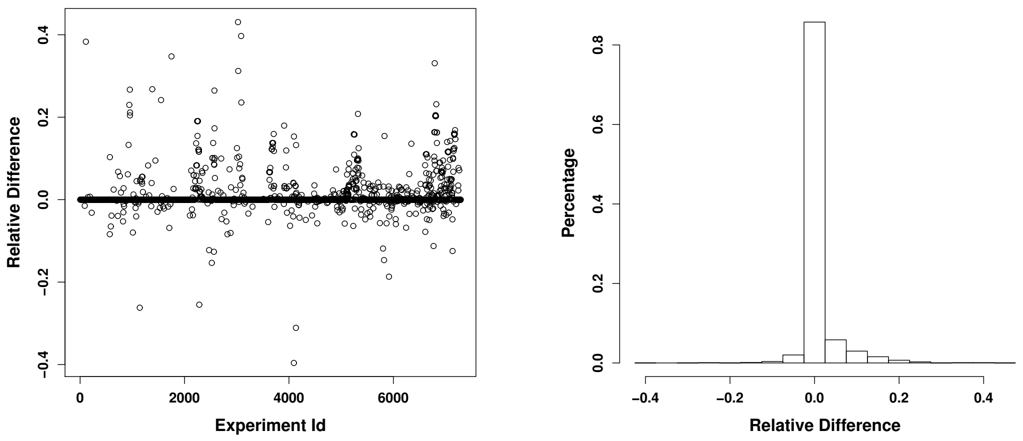

Figure 2.6: Result overview of all experiments.

Scheduler	*No change*	*Early better*	*Late better*	*Average improvement*	*Average degradation*
MCT	74.5%	15.9%	9.5%	8.2%	-6.7%
HEFT	89.3%	10.1%	0.5%	10.9%	-5.6%
PEFT	84.5%	12.2%	3.3%	10.2%	-5.8%
Lookahead	84.9%	12.6%	2.5%	8.8%	-5.1%
Min-Min	89.6%	9.3%	1.1%	10.7%	-5.6%
Max-Min	87.9%	10.7%	1.4%	8.6%	-18.2%
Sufferage	89.3%	10.2%	5.5%	9.2%	-11.4%

Table 2.3 Results by scheduler type.

performance improvement of 9.4%, and the experiments for which is slower show an average performance degradation of -7.3%.

These results indicate that for the majority of workflows, using early or late evaluation mode has practically no significant impact on scheduling performance. Only for a minority of 10%, the executed workflows in early enactment mode caused a performance improvement of 10%. It is also observed that 3% of the workflows executed in early enactment mode led to worse performance. The reason for this result is that the schedulers are suboptimal heuristics and that more but still incomplete information can still cause the scheduler to misjudge the critical path (see Section 2.2.5), while with less information the scheduler may correctly guess the critical path.

Table 2.3 and Figure 2.7 show the experimental results by scheduler type. MCT schedules activities to the fastest available machine as they are passed to the scheduler and it does not take the rest of the WEP into account. Therefore, it is the least stable, and its results roughly form a Gaussian distribution. However, MCT still shows a slight bias towards early evaluation mode, 6% more workflows showing better performance. The full-ahead scheduler shows rather stable performance with 80%-90% of the workflows having no significant performance difference between early

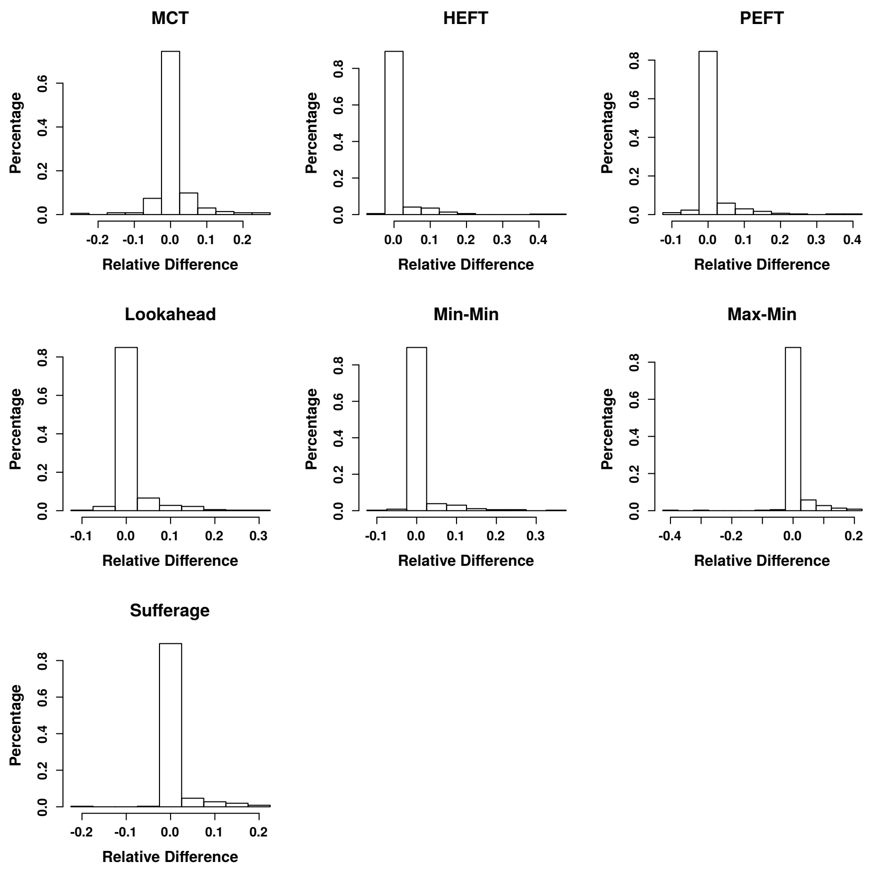

Figure 2.7: Histograms of relative performance by scheduler type.

Hardware config	*No change*	*Early better*	*Late better*	*Average improvement*	*Average degradation*
Config 1	84.2%	12.1%	3.7%	9.3%	-7.8%
Config 2	84.3%	12.1%	3.6%	9.5%	-7.5%
Config 3	84.2%	12.6%	3.2%	9.2%	-7%

Table 2.4 Results by hardware configuration.

and late evaluation mode. For the workflows where there is a significant performance difference, it is early evaluation mode showing a better performance in the majority of cases. The only exception is Sufferage, where only twice as many workflows show better performance with early evaluation mode.

Table 2.4 and Figure 2.8 show the experimental results by the hardware configuration. There is no significant difference in the results for the different hardware configurations. For all hardware configurations, 84% of all experiments show no significant difference between early and late evaluation mode, 12% show 9% better performance with early evaluation mode, and 4% show 7% of worse performance.

Table 2.5 and Figure 2.9 show the experimental results by workflow shape α. Also here, there is hardly any difference between different workflow shapes. For all workflow shapes, 84% of the experiments show no significant difference between early

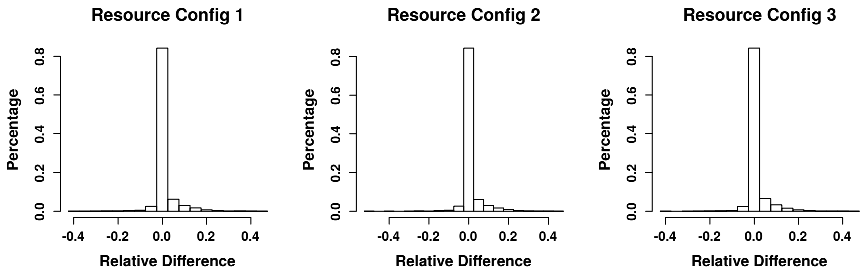

Figure 2.8: Histograms of relative performance by hardware configuration.

Workflow shape	*No change*	*Early better*	*Late better*	*Average improvement*	*Average degradation*
0.1	85.8%	11.4%	2.8%	9.3%	-7.1%
0.5	86.2%	10.8%	3%	9.3%	-7.4%
1.0	83.7%	13.2%	3.1%	13.2%	-3.1%
1.5	83.9%	12.5%	3.6%	9.2%	-7.4%
2.0	84.4%	12.1%	3.5%	9.2%	-7.9%

Table 2.5 Results by workflow shape α.

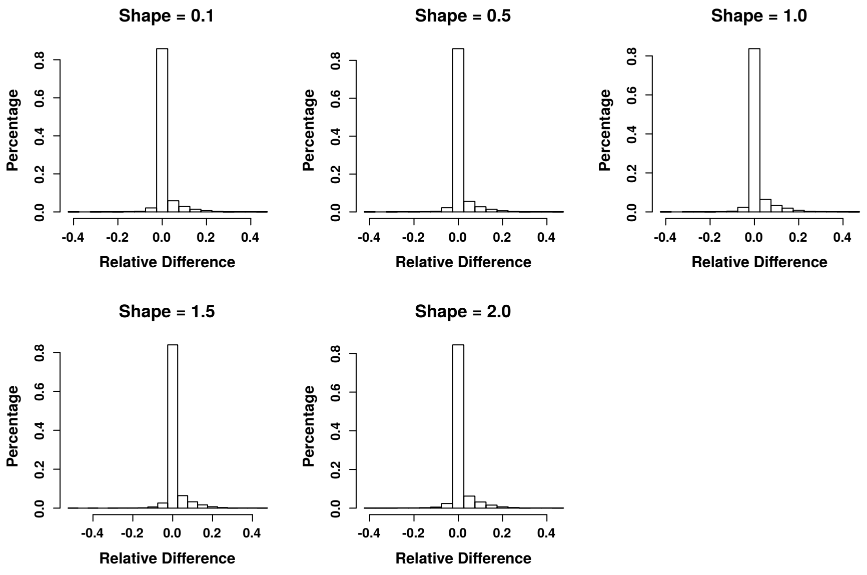

Figure 2.9: Histograms of relative performance by workflow shape α.

and late evaluation mode, 12% show 9% better performance with early evaluation mode, and 3% show 7% of worse performance. The only difference is $\alpha = 1.0$, which shows an average performance improvement of 13.2% instead of 9%, and an average performance degradation of -3.1% instead of -7%. For $\alpha = 1.0$, the workflow height and width is the same, which means that all activities are equally distributed. This gives the scheduler the most opportunities for improving the mapping.

Table 2.6 and Figure 2.10 show the experimental results concerning the output degree of workflow activities. Also here there is hardly any difference between

Outdegree	*No change*	*Early better*	*Late better*	*Average improvement*	*Average degradation*
1	84.4%	11.8%	3.8%	9.1%	-6.9%
3	83.8%	12.8%	3.4%	9.5%	-7.4%
20	84.6%	12.1%	3.3%	9.3%	-8.2%

Table 2.6 Results by outdegree.

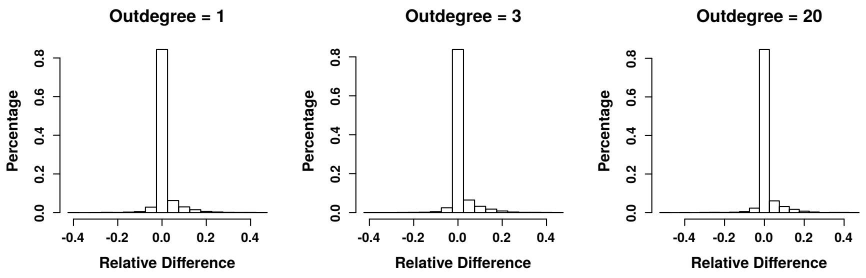

Figure 2.10: Histograms of relative performance by outdegree.

different output degrees. For 84% of the experiments there is no significant difference between early and late enactment mode, for 12% of the experiments early enactment mode causes 9% of better performance, and for 3% of the experiments the early enactment mode causes 7% of worse performance.

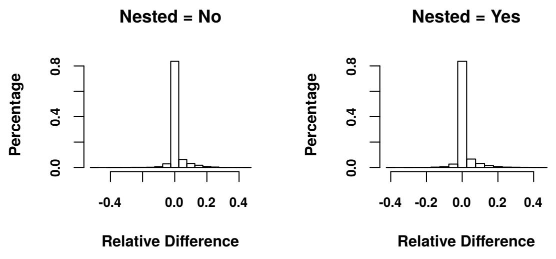

Figure 2.11: Histograms of relative performance by composite nesting level.

Table 2.6 and Figure 2.10 show the experimental results considering whether there is nested composite activities in the workflow. Also here, there is hardly any difference, 84% showing the same performance, 12% showing better performance with early enactment mode with a performance improvement of 9% and 3% show 7% of worse performance.

2.2.8 *Conclusion*

The impact of early and late enactment modes on workflow execution performance were evaluated. Early evaluation mode provides more information to the scheduler, which can calculate a potentially better schedule, improving the workflow performance. On the other hand, early evaluation mode causes a significant increase in workflow enactment overhead degrading workflow execution performance and limit-

Nested	*No change*	*Early better*	*Late better*	*Average improvement*	*Average degradation*
No	83.7%	12.4%	3.9%	9.3%	-7.9%
Yes	83.6%	12.7%	3.7%	9.3%	-7%

Table 2.7 Results by composite nesting level.

ing scalability. In order to find guidelines to when early evaluation mode significantly improves workflow performance, results were broken down according to several parameters defining workflow shape and structure.

The first relevant result is that for 85.7% of the experiments we could not find a significant difference in workflow performance between early and late execution mode. We conclude that it is safe to use late evaluation mode for most workflows to get better scalability and less enactment overhead without the fear of loosing performance because of a suboptimal workflow schedule. Only for 11.6% of the experiments we observed a significantly better performance with early enactment mode with an average improvement of 11.6% and a maximum improvement of 43%. For 2.7% of the experiments, we observed a significantly worse performance with early evaluation mode with an average performance degradation of 7.3% and a maximum performance degradation of 39.6%.

The second relevant result is that for 14.3% of the experiments, while there is a significant difference in performance between early and late enactment mode, no decisive guidelines were identified when a workflow performs better. The best enactment mode is highly individual for each workflow and no correspondence can be made to a specific parameter defining workflow shape or structure. The only way to determine whether early or late enactment will cause a better performance is to execute the workflow using both modes and compare the results.

Based on these results, the late enactment mode was selected as the default mode in MWRE. According to the experiments, the potential performance improvement of early enactment mode due to a better scheduling is too insignificant compared to the downsides of a higher enactment overhead and worse scalability.

MWRE is a workflow engine for shared-memory heterogeneous manycore computers, and thus, MWRE workflows have different characteristics than DCI (Cloud) workflows. More precisely, they feature a more complex workflow structure with a higher number of shorter running activities. The experimental results reflect this and, therefore, only have limited validity for common DCI environments. Because DCI workflows have a simpler structure with a lower number of longer running activities, the early evaluation mode here has less impact on scheduling performance.

2.3 Towards General Purpose Computations at the Edge

Originally designed to exploit the power of multi-core processors through virtualization, Cloud Computing [93] has changed over the past decade to support ultrascale computations. The new paradigm, often called *aggregation*, collects a large number of resources in a pool to form a single service with huge storage and computation capacities. Unfortunately, with the huge amounts of data generated via modern applications, the cloud center has become a bottleneck and a single point of failure. This advocated an extended paradigm, called *Edge Computing*, that brings part of the data storage and computation closer to the user. The benefits are plenty: reduced delays, high availability, low bandwidth usage, improved data privacy, etc. In this section, we introduce recent advances in edge computing that makes the coordination of edge networks synchronization-free and convergent. We address the main challenges facing applications on the data management and communication aspects. The section also provides convenient runtime environments for different categories of edge computing scenarios[16].

2.3.1 Motivation

Edge Computing offers the opportunity to build new and existing ultrascale applications that take advantage of a large and heterogeneous assortment of edge devices and environments. Fully realizing the opportunities that are created by edge computing, requires dealing with a set of key challenges related with the high number of different components that compose such systems and the interactions among them. In this work, was address the main challenges on the communication and data management levels allowing for robust communication and available data access.

On the communication frontend, the fact that applications are composed of components running in heterogeneous environments requires robust and efficient solutions for tracking these components. This implies the development of highly robust and adaptive membership services and mechanisms that allow efficient communication among these components. Among the promising class of gossip-based communication protocols are those "hybrid" ones [94, 95], in which payloads are propagated though an elected logical *spanning tree*, supported by lightweight meta-data across the graph for recovery (reconstructing another logical tree) under failures.

The consequences of such hostile environments are also present on the data management level. Since application components run on different administrative domains scattered across heterogeneous environments, communication links between these components can be disrupted by external factors (i.e, network partitions) frequently. This implies that the progress of computations executed across different application components cannot depend on continuous communication with other components, or in other words, cannot depend on synchronous interactions. This advocates the use of synchronization-free (i.e., sync-free) programming abstractions backed by sync-free data propagation and replication techniques. An interesting approach is to make use of Conflict-free Replicated Data Types (CRDTs) [96, 97, 98] that are proven abstractions designed to achieve convergence under such conditions (this is explained later in more details).

[16]Credits go to all team members contributed to the success of this work within the EU FP7 Syncfree project and EU H2020 LightKone project. The research leading to these results has received funding from the European Union's Horizon 2020 - The EU Framework Programme for Research and Innovation 2014-2020, under grant agreement No. 732505, LightKone project.

Finally, heterogeneity is the norm in ultrascale edge applications, and it exists at various layers: execution environments, communication media, data sources, operating systems, programming languages, etc. Addressing this heterogeneity can be achieved by leveraging on different run-time supports and frameworks that provide a more unified vision of resources to application developers. These different run-time and frameworks will have to inter-operate through the use of standard protocols and common data representation models.

In the following we refine the challenges associated with tapping on edge computing to design ultrascale applications, and discuss enabling technology that paves the way to tackle these challenges, and finally discuss a set of run-time and framework support that can simplify the design of such applications.

2.3.2 Edge Computing Opportunities

Edge Environments. To the contrary of cloud computing where the data and computation is centralized at the cloud data centers, the edge computing paradigm encompasses a large number of highly distinct execution environments that are defined by the network topology, connectivity, locality, and the storage and computation capacities of the devices used. In particular, we identify we identify the following interesting edge environments:

- Fog Computing: a variant of cloud computing where the cloud is divided into smaller cloud infrastructures located in the user vicinity. In such environments, each fog cloud often serves as an individual cloud, although the data can eventually be incorporated with other fog [99, 100].
- Mobile Cloudlets: small cloud datacenters that are located at the edge and are tailored to support mobile applications with powerful computations and low response times, e.g., in ISP gateways or 5G towers [101, 102, 103].
- Hardware-based Clouds: self-contained devices, such as routers, gateways, or set-up boxes, that are enriched with additional computational and storage capabilities like [104, 105].
- Peer-to-Peer (P2P) Clouds: these environments try to leverage existing devices, e.g., user mobiles, laptops, and computers in volunteer networks, aiming to cooperate towards achieving a common goal [106, 107, 94].
- Things and Sensor Network Clouds: resource constrained devices, e.g., Internet of Things devices, sensors, and actuators, capable of performing some computations on data without accessing or delegating to the (possibly unreachable) cloud center [108].

All of these different scenarios are characterized by having highly heterogeneous devices in terms of processing power and memory, but also regarding their connectivity to the backbone of the Internet or even their up-times (being continually running or being operating for only small periods of time). These different devices naturally, run different operating systems, from general purpose Linux based operating systems in the case of servers in cloud and private infrastructures, to proprietary operating systems in the case of set-up boxes, mobile operating systems, general purpose multi-user operating system or even single process operating systems in the case of small sensors and actuators. Gathering the capacity of devices with very different properties is highly challenging, and devising solutions that can exploit devices located in different edge devices brings additional challenges. Next we will discuss some of the key high level challenges in tapping the potential of the edge.

Challenges at the Edge Despite the diversity of edge computing environments, components, and properties, the major challenges are common to most of the scenarios. In particular, we recognize the following four challenges:

Scalability. One of the reasons to move the data and computation off the cloud data center to the edge is to reduce the I/O overload on the cloud and avoid bottlenecks related with the limited network capability connecting clients to the cloud infrastructures. Nevertheless, this raises another challenges on handling the data and computation in a distributed way especially in ultra-scale systems composed of, potentially, many data centers and thousands of edge devices. This scale requires special techniques across the data, computation, and communication planes. As captured by the CAP theorem [109], and because scaling out will increase the potential for network portions, link failures, and arbitrary communication delays, ensuring availability—as an essential requirement for most applications including novel edge applications—requires relaxing the consistency model employed in the design and implementation of these solutions. Consequently, the computation should also be decentralized and coordinated to achieve the common goals of the entire system. Finally, the communication middlewares should also scale to afford a high number of nodes, e.g., through asynchronous, P2P, or gossip protocols.

Interoperability. Considering the edge categories discussed above, one can notice the notable diversity level of the devices and platforms used within the same or across edge clouds. This brings interoperability challenges if all components shall communicate with each others, thus requiring well studied interfaces and possibly introducing a common layer that all components can understand without compromising the characteristics deemed essential.

Resilience. While cloud datacenters use high quality equipment for the network and devices, edge computing often use commodity equipment that are far from perfect regarding failures. The problem is extrapolated with edge network problems that are likely to be loosely connected, mobile, and hostile. This threatens the quality of the service and makes the data and communication components even more complex. That said, one must consider the performance as well as the cost trade-offs (being a major factor due to the constrained resources).

Security and Privacy. Given the heterogeneity of the edge applications, security and privacy measures must be analyzed and tackled individually. However, in general, it is desired to find a common security layer or security measures that govern a wide range of applications. Security and privacy on the edge need to be addressed on the infrastructure and data levels. The former can be deployed at the communication or network layer, ranging from establishing secure connections to enforcing secure group dynamics, and cover several dimensions including data integrity, data privacy, or resilience to DoS attacks. On the other hand, edge applications often deal with sensitive data which likely requires lightweight encryption and data sanitization techniques to control the disclosure of such data. These may also include secret-sharing, anonymization, noise addition or partitioning, etc., depending on the specific security and functional requirements of the implementations.

Use Cases. As discussed in the edge environments, edge computing supports a plenty of applications and use-cases. In this section, we focus on three categories in which most of the use-cases lie:

- Time series applications. This category spans a multitude of applications with the popularity of IoT. The scenario is often a type of time series where data is generated by the IoT devices, e.g., sensors, and pushed to the edge devices to get stored, aggregated, and partially computed. The aggregated data is then pushed to the center of the cloud for further handling. The data-flow can sometimes be in the opposite sense if actuator devices exist; in this case, the processed data in the cloud is pushed back to the actuators to do some action. Consequently, this scenario represents a hybrid model of light and heavy devices, different types of networks (e.g., Zig-bee, WIFI, WAN, etc), as well as data-flow direction.
- Mobile edge applications. This category covers all the applications in which devices are mobile and public. This makes the model very hostile as link failure and delays are expected, and the availability of nodes cannot be guaranteed (e.g., a mobile device can be switched off). The communication in such use cases does not follow a particular data-flow pattern, but it is often P2P or gossip-based due to the dominant dynamic graph-like network of nodes. In such applications, devices have moderate storage and computation resources that makes the interaction symmetric. Obviously, the main challenges in such use-cases are reseliance and availability. In some cases, access points, towers, or routers with more capacities can assist in storage, computation, and communication, which can be used as third party authority when needed.
- Highly available databases. This category is a natural evolution of scalable databases in cloud and cluster systems. The intuition is to replicate the database geographically, brining replicas or cache servers closer to the user. In this scenario, devices are at least commodity computers or servers with non-scarce capacities, and then network is often the Internet. In addition to availability, the challenge in such use-cases is to tolerate network partitions and optimize data locality (especially when partial replication is used). These scenarios are close to Fog Computing and Cloudlets with the difference that all node must work as a single (often loosely) coordinated system.

2.3.3 Enabling Technologies for the Edge

Synchronization-Free Computing. Edge devices and edge networks are both unreliable. This follows both from their design, e.g., they are low-power systems that are often offline, and from the nature of the edge itself, e.g., it is directly involved with real world activities, such as in Internet of Things. Despite this unreliability, we would like to perform computations directly on the edge.

To perform computations directly on the edge, we need distributed data structures and operations that tolerate the unreliability of the edge. Synchronization-free computing fits the bill because of its very weak synchronization requirement. A prominent example is Conflict-free Replicated DataType (CRDT), which is a replicated data type that is designed to support temporary divergence at each replica, while guaranteeing that when all updates are delivered to all replicas of a given instance, they will converge to the same state. (More details about CRDTs can be found in Chapter 4 or by referring to [96, 97, 98].) CRDTs naturally tolerate node problems, namely nodes going offline and online and node crashes, and network problems, namely partitions, message loss, message reordering, and message duplication. Node crashes are tolerated as long as the desired state exists on at least one correct node. The following results on CRDT computations are summarized from [110].

CRDT Definition. For the purposes of this section, we define a *CRDT instance* to be a replicated object that satisfies the following conditions:

- Basic structure: It consists of n replicas where each replica has an initial state, a current state, and two methods, query and update, that each executes at a single replica.
- Eventual delivery: An update delivered at some correct replica is eventually delivered at all correct replicas.
- Termination: All method executions terminate.
- Strong Eventual Consistency (SEC): All correct replicas that have delivered the same updates have equal state.

This definition is slightly more general than the one given in the original report on CRDTs [96]. In that report, an additional condition is added: that each replica will always eventually send its state to each other replica, where it is merged using a join operation. This condition is too strong for CRDT composition, since it no longer holds for a system containing more than one CRDT instance. We explain the conditions needed for CRDT composition in the next section.

CRDT Composition. The properties of CRDTs make them desirable for computation in distributed systems. It is possible to extend these properties to full programs where the nodes are CRDTs and the edges are monotonic functions. To achieve this, it is sufficient to add the following two conditions on the merge schedule, i.e., the sequence of allowed replica-to-replica communications:

- Weak synchronization: For any execution of a CRDT instance, it is always true that eventually every replica will successfully send a message to each other replica.
- Determinism: Given two executions of a CRDT instance with the same set of updates but a different merge schedule, then replicas that have delivered the same updates in the two executions have equal state.

The first condition allows each CRDT instance to send the merge messages it requires to satisfy the CRDT conditions. The second condition ensures that the execution of each CRDT instance is deterministic, which makes it a form of functional programming. We remark that SEC by itself is not enough for this, since the states of replicas *in different executions* that have delivered the same updates can be different, even though SEC guarantees that they are equal in the same execution. In practice, enforcing determinism is not difficult but it depends on the type of the CRDT instance. Article [110] explains how to do it for a set that has add and remove operations (the so-called Observed-Remove Set).

We define a *CRDT composition* to be a directed acyclic graph where each node is a CRDT instance, and each node with at least one incoming edge is associated to a function of all incoming edges arranged in a particular order. Given the first of the two conditions introduced above, we can show that the execution of a CRDT composition satisfies the same properties as a single CRDT instance. If the second condition is added, then the CRDT composition behaves like a functional program.

Hybrid Gossip Communication. Gossip is a well known and effective approach for implementing robust and efficient communication strategies on highly dynamic and large-scale system [107, 95]. In its most simple form, in a gossip protocol, each node periodically interacts with a randomly selected node. In this interaction both exchange information about their local state (and potentially merge it). Since all nodes do this in parallel and in an independent fashion, after approximately one round-trip time, all nodes will have performed, at least, one merge step, and on average two merge steps (one initiated by the node itself and another initiated by some peer). We usually call this period of interactions a *cycle*. After a small number of cycles, the network converges to a globally consistent vision of the system state. This simple approach cab be used, for instance to compute aggregate functions, such as inferring the network size or load. Interestingly, this can also be used for other, and more complex, purposes such as managing the membership of large-scale system, which implies building and maintaining an overlay (i.e, logical) network topology, in a way that is both robust and scalable, but also to support robust data dissemination in such systems.

Gossip-based approaches have been shown to be highly resilient to network faults, due to the inherent redundancy that its core to the design of gossip protocols. Unfortunately, this redundancy also leads to efficiency penalties. Hybrid gossip addresses this aspect of gossip protocols. In a nutshell, the key idea of hybrid gossip is to leverage on the feedback produced by previous gossip interactions among nodes, such that an effective and non-redundant structure of communication can naturally emerge. The topology of this *emergent structure* depends on the computation being performed by nodes, and it enables nodes significantly improve the communication and coordination cost by restricting the exchange of information among node to the logical links that belong to this structure, lowering the among of redundant communication.

Key to maintaining the fault-tolerance of gossip protocols in hybrid gossip is the use of the remaining communication paths among nodes (those that are not selected to be part of the emergent structure) to convey minimal control information. This control information enables the system to detect (and recover) from failures that might affect the emergent structure. Moreover, in highly dynamic scenarios, the additional communication paths allow nodes to fall back to a pure gossip strategy, for instance, when there are a significant number of concurrent nodes crashes or network failures.

Interesting, hybrid gossip solutions naturally allow different components of the system to operate using either the emergent structure or a pure gossip approach simultaneously. Hence, components of the system that are in stable conditions (i.e, low membership dynamics and low failures) will operate resorting to the emergent structure, while components of the system that are subjected to high churn or network/node failure will fallback to use pure gossip while still being able to inter-operate with the components using the emergent structure.

Therefore, hybrid gossip approaches enable applications to, effectively and transparently, benefit from the resilience of a pure gossip approach entwined with the efficiency of a gossip approach that leverages an emergent communication topology. The hybrid gossip approach has been introduced in [94, 111]. The Plumtree protocol in particular, shows how to build an efficient and robust spanning tree connecting large number of nodes to support reliable application-level broadcast. This solution is currently used in industry, for example, the Basho Riak database uses it to manage the underlying structure of its ring topology which is used to map data object keys into nodes (through consistent-hashing).

2.3.4 Runtime for Edge Scenarios

Above we have discussed enabling technologies that can be leveraged to build new and exciting edge applications in the ultrascale domain. Tapping into these enabling technologies can however, be a complex task for developers. Therefore, it becomes relevant to provide frameworks, tools, and other artifacts that exploit these technologies in a coherent way, providing high level abstractions to programmers that aim at developing their ultrascale edge applications. We now discuss some existing runtime support tools and frameworks that have been recently proposed to this end.

Antidote. Antidote is a geo-replicated key-value store, designed for providing strong guarantees to applications while exhibiting high availability, thus providing a good compromise in the consistency versus availability trade-off in the design of cloud databases. These proprties make Antidote a strong candidate as an edge database especially when edge nodes have non-scarce resources (e.g., commodity servers).

In particular, some cloud databases adopt a strong consistency model by enforcing a serialization in the execution of operation, leading to high latency and unavailability under failures and network partitions. Other databases adopt a weak consistency model where any replica can execute any operation, with updates being propagated asynchronously to other replicas. This approach leads to low latency and high availability even under network partition, but replicas can diverge. On the other hand, Antidote allows any operation to execute in any replica, but provides additional guarantees to the application as we explain next.

First, Antidote relies on CRDTs for guaranteeing that concurrent updates are merged in a deterministic way. Antidote provides a library of CRDTs with different concurrency semantics, including registers, counters, sets and maps. The applications programmer must select the most appropriate CRDT, considering its functionality and concurrency semantics (e.g., add-wins, remove-wins).

Second, Antidote enforces causal consistency, guaranteeing that whenever an update u may depend on update v, if a client observes update u he also observes update v. Applications can leverage this property to guarantee their correctness when the correctness depends on the order of updates, e.g., an update executed after changing the access control policies should not be visible in a replica with the old access control policies.

Third, Antidote provides a highly available form of transactions, where reads observe a causally-consistent snapshot of the database and writes are made visible atomically. Unlike standard transactions, write-write conflicts are solved by merging the concurrent update. Applications can leverage these highly-available transactions to guarantee that a set of updates is made visible atomically.

Fourth, Antidote provides support for efficiently enforcing numeric invariants, such as guaranteeing that the value of a counter remains larger than 0. To this end, it includes an implementation of a Bounded Counter CRDT [112], a shared integer that must remain within some bounds. The implementation uses escrow techniques [113] for allowing an operation to execute in a replica without coordination in most cases.

Finally, associated with Antidote, we have developed a set of tools to verify whether an application can execute correctly under weak consistency, and when this is not the case, what coordination is necessary. These tools are backed by a principled approach to reason about the consistency of distributed systems [114].

Antidote is designed to be deployed in a set of geo-distributed data centers. Within each cluster, data is sharded among the servers. Data is geo-replicated across data centers. The execution of transactions in Antidote, and the replication of updates across data centers, is controlled by Cure [115], a highly scalable protocol that enforces transactional causal+ consistency (combining CRDTs for eventual consistency, causal consistency and highly available transactions).

Legion. Legion [2] is a new framework for developing collaborative web applications that transparently leverage on the principles of edge computing by enabling direct browser-to-browser communication. Legion was implemented in *javascript* and it uses the *Web Real-Time Communications* (https://webrtc.org) to establish direct communication channels among web application users. At its core, Legion enables applications to transparently replicate, in the form of CRDTs, relevant application state in clients. Clients can then modify the application state locally, and through the use of hybrid gossip mechanisms, synchronize directly among them, without the need to go through the web application server. The server however is still used both to ensure the durability of the application state, but also to assist in the operation of Legion, namely to simplify the task of creating the initial webRTC connections among clients when they enter the application.

A simplified architecture of Legion is illustrated in Figure 2.12. Legion can be used by a web application simply by importing a javascript script. This script provides the application access to the *Legion API*. The API exposes to the application the ability to manipulate data objects that can be used to model the application state. These data objects include records, counters, lists, and maps. All of these objects

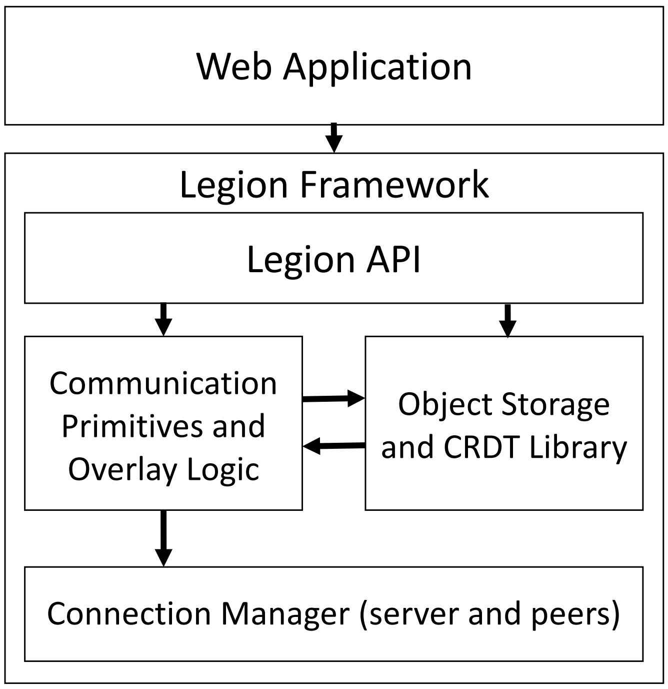
Web Application
Legion Framework
Legion API
Communication Primitives and Overlay Logic
Object Storage and CRDT Library
Connection Manager (server and peers)

Figure 2.12: The Legion architecture (adapted from [2])

are internally represented by Legion through CRDTs which simplifies the the direct synchronization among clients of shared application state. This is provided by an extensible CRDT Library that is part of the *Object Store* component of Legion . The synchronization of objects among clients (and that of a subset of clients with the server to ensure durability) is transparently managed by the Object Store.

To guide the synchronization process, Legion leverages on an unstructured overlay network, whose construction is guided by the principles of hybrid gossip, and takes into consideration the relative distance of each client among them. This allows clients to mostly interact and synchronize with clients that are in their vicinity. While the typical use case in Legion is to have clients interacting through the manipulation of shared data objects, web applications also have access to communication primitives that enable them to disseminate messages among the currently active clients of the application in a decentralized fashion. This is achieved by a gossip-based broadcast protocol that operates on top of the legion overlay network.

Finally, Legion also takes into account security, by ensuring that before clients can start to replicate and manipulate application data objects they authenticate on a server. Moreover, Legion exposes an adapter API, that allows developers to integrate their Legion-backed applications with existing backends. The framework provides adapters to the Google Real Time API[17]. These adapters allow the developers to leverage this backed to do any combination of the following: authentication and access control, data storage for durability, and support to the WebRTC signaling protocol required to create webRTC connections among browsers. More details on the design and operation of Legion can be found in [2]. Legion is open source and available, along side some demo applications through https://legion.di.fct.unl.pt.

[17]https://developers.google.com/google-apps/realtime/application

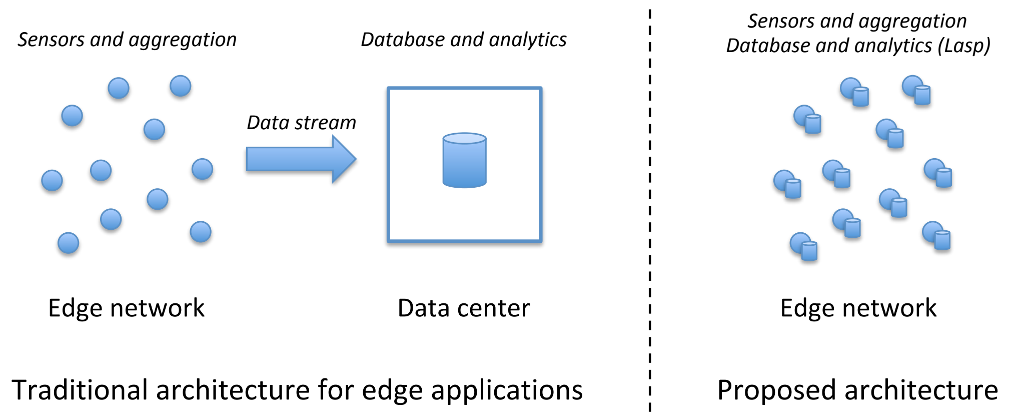

Figure 2.13: Proposed architecture for edge applications using Lasp

Lasp. The Lasp language and programming system [116] was designed for application development on unreliable distributed systems, and in particular for edge computing. Lasp allows developers to write applications by composing CRDTs, as explained above [110]. In addition to composition, Lasp also provides a monotonic conditional operation that allows executing application logic based on monotonic conditions on CRDTs. The Lasp implementation combines a programming layer based on synchronization-free computing with a communication layer based on hybrid gossip. This makes the implementation highly resilient and well-adapted to edge networks.

Many of today's edge applications use the cloud as a database to store data coming from the edge. By using Lasp as their database, such applications can be translated to fully run on the edge (see Figure 2.13). This cannot be done with traditional cloud databases since they are not designed to run on unreliable edge networks. In the proposed architecture, the edge network runs everything: the sensors and aggregation software on individual edge nodes, and the database (Lasp) on all edge nodes. Analytics computations can be run either as an internal Lasp computation or external to Lasp on individual nodes, using Lasp just as a database.

Example Lasp program. A typical application for Lasp is the scenario of advertisements counter that counts the total number of times each advertisement is displayed on all client mobile phones, up to a preset threshold for each. Figure 2.14 defines graphically part of the Lasp program for this application. The actual code is a straightforward translation of this graph. The application has the following properties:

- Replicated data: Data is fully replicated to every client in the system. This replicated data is under high contention by each client.
- High scalability: Clients are individual mobile phone instances of the application, thus the application should scale to millions of clients.
- High availability: Clients need to continue operation when disconnected as mobile phones frequently have periods of signal loss (offline operation).

This application can be implemented completely on the edge, as explained previously, or partly on the cloud. For this application we have demonstrated the scalability of

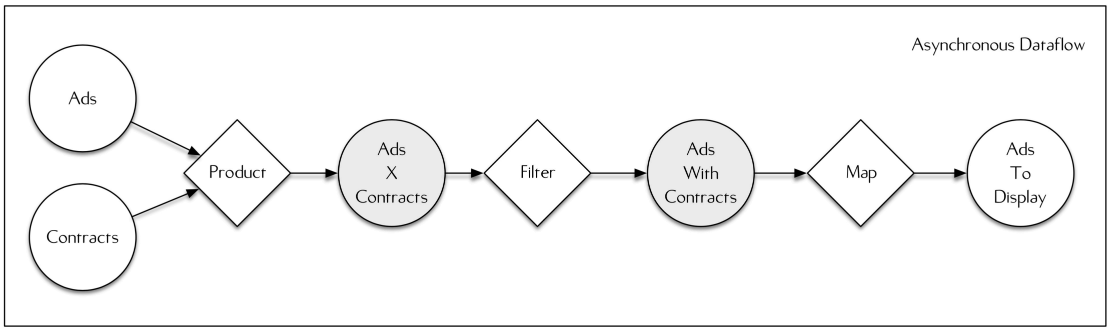

Figure 2.14: A Lasp computation to derive the set of displayable advertisements in the advertisement counter scenario. On the left, Ads and Contracts give information for the advertisements, including how many times they have been displayed, and their contracts, including the threshold for each advertisement. On the right are the advertisements that can be displayed. All data structures are sets, similar to database relations, and the computation is similar to an incremental SQL query.

the Lasp prototype implementation up to 1024 nodes by using the *Amazon* cloud computing environment to simulate the edge network [117].

2.3.5 Future Directions

Building additional tools and support for a new generation of ultrascale edge applications is quite relevant and challenging. The varied nature of edge computing environments, which can combine small private clouds and data centers, specialized routing equipment and 5G towers, users desktops, laptops and even cellphones, to small things sensors and actuators, makes it a daunting task to build a single runtime support that can efficiently operate on all such devices and deal with their heterogeneity.

While we presented a set of tools and frameworks that can ease the development of ultrascale edge computing applications and services, these do not cover all possible execution scenarios. That path to build such support requires not only the development of specialized runtimes for different edge settings, but also devising standard protocols and data representation models that allow the natural integration of different runtimes in a cohesive and effective edge architecture.

Current solutions for data replication and management are also unsuitable for the ultrascale that one is expected to find in emerging edge computing applications. The use of CRDTs to address the requirements of data management in this setting presents a viable approach. However, further efforts have to be dedicated in designing new and efficient synchronization mechanisms that can naturally adapt to the heterogeneity of the execution environment.

2.4 Spectral Graph Partitioning for Process Placement on Heterogeneous Platforms

It is customary in the literature to model a distributed application as a graph, whose vertices are processes, or computing tasks, and an edge between tasks denotes a communication between them. The edges are weighted with a positive value to mark the magnitude of this communication. Frequently used magnitudes to measure the communications are the data volume, in total number of bytes, or the number of messages interchanged [118].

In this setting, spectral techniques divide the set of vertices in two parts, equal in number of vertices, in such a way that the total communications from one part to the other is lesser than between the two parts of any other partition. The practical interest for this is to assign each part to a computation node, so the slow communication link between two nodes are used less than the quick intra-node links. It is imposed that the computational nodes are similar in performance, and also similar the computational requirements of the vertices, in order for the assignation be balanced. The theoretical resource that allows to compute this in an effective way is the Fiedler eigenvector of the Laplacian matrix of the graph [119]. The study of the eigenvalues and eigenvectors of a matrix is called spectral resolution [120], hence the name of the method.

In this subsection we describe the spectral method as it is customarily used. We also propose to extend the previous scheme in two directions. First, we consider that each vertex has assigned a volume or weight, positive but possibly different depending on the vertex. To divide the set of vertices into two parts, so that the part have the same volume (possibly with different number of vertices), we consider the Fiedler eigenvalue of a generalized Laplacian (that we will define) which has similar properties to the standard Laplacian. The practical interest of this extension comes from the fact than the computational requirements of each vertex (process) can be different, and we are interested in a partition in vertex subsets with equal computational load (not necessarily equal number of vertices).

A second extension is to consider the division in two parts, where the fraction of total volume assigned to each part is not the same, but can be predefined to p and $1-p$ to each part, for a fraction p of the total of vertices. The Fiedler eigenvector of the generalized Laplacian can be used to this end. This is of interest for the case where the two subsets of vertices/processes will be assigned to computational units that are not equal in speed, being instead proportional to p and $1-p$. Hence, the partition of tasks is conformal with the speed of the intended processors. We also discuss the problem of partitioning in more than two parts. We find difficult to put it in this scheme.

For the structure of the subsection, in the following subsubsection we describe notation about graphs and Linear Algebra. Then we introduce the Spectral Partitioning technique using the Laplacian . The material is standard but our presentation emphasizes the operator view (that is, avoid references to coordinates as much as possible). The subsubsection 2.4.3 is our work about weighted graph partitioning using a potential over the vertices. We use a finite element model as example. After a numerical comparison of performance against other partition methods, using the software Scotch, we draw some conclusions.

2.4.1 Graphs and Matrices. Examples

A graph $G = (V,E)$ consists of a set V of *vertices*, and a set E of *edges*, being each edge a set $\{u,v\}$ of two vertices $u,v \in V$. Each edge $\{u,v\}$, also noted $u \sim v$, is said that joins u and v. Note that this structure does not models loops or directed arrows.

A *weight on edges* is a map

$$w : E \to \mathbb{R}.$$

The weight of the edge $u \sim v$ is denoted $w(u,v)$. If a weight on the edges is not specified, implicitly the constant unit weight must be considered (that is, $w(u,v) = 1$ for each $(u \sim v) \in E$).

The *degree* of a vertex is the number of vertices adjacent to it.

A *potential on vertices* is a map

$$p : V \to \mathbb{R}.$$

The set of all potentials (that is, of all functions $V \to \mathbb{R}$) is denoted $\mathbb{R}^V$.

We choose an ordering of the set of vertices, $V = \{v_1, \dots, v_n\}$. The *adjacency matrix* of G (for this conventional ordering) is the $n \times n$ symmetric matrix A:

$$A = \begin{pmatrix} a_{11} & a_{12} & \cdots & a_{1n} \\ a_{21} & a_{22} & & a_{2n} \\ \vdots & & \ddots & \vdots \\ a_{n1} & a_{n2} & \cdots & a_{nn} \end{pmatrix} \text{ with } a_{ij} = \begin{cases} 1 & \text{if } v_i \sim v_j \\ 0 & \text{if not} \end{cases} \quad \text{for } i,j \in \{1, \dots, n\}.$$

For a edge weight w, its *weighted adjacency matrix* is A_w with entries a_{ij} where

$$a_{ij} = \begin{cases} w(v_i, v_j) & \text{if } v_i \sim v_j \\ 0 & \text{if not} \end{cases}$$

The adjacency matrix is the matrix of the constant unit weight $w(u,v) = 1$ if $u \sim v$. We will consider mainly *positive edge weights* (that is, weigths w such that $w(u,v) > 0$ for each $(u \sim v) \in E$), with the notable exception of the Laplacian.

We represent a vertex potential $p : V \to \mathbb{R}$ as the vector $p = (p(v_1), p(v_2), \dots, p(v_n))$. A weighted adjacency matrix A_w operates in $\mathbb{R}^V$, the set of vertex potentials, as a matrix multiplication.

$$\begin{aligned} A_w : \mathbb{R}^V &\longrightarrow \mathbb{R}^V \\ p &\longmapsto A_w p \end{aligned}$$

That is, the vector $A_w p$ has as j-entry the value $\sum_{j=0}^{n} a_{ij} p(v_j)$.

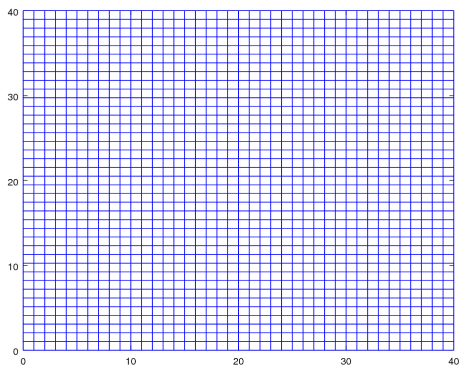

Figure 2.15: Square mesh of size 40×41

To give an intuitive interpretation of this setting, we consider a easily visualizable graph: the vertices are a square lattice of dots, and four edges join each one with those placed up, down, left and right (three edges for lateral vertices and two for the corners, figure 2.15). This type of graph is used in finite elements computations. It is symmetric.

As example of weight in this graph, let's take that each edge has weight one, so $A_w = A$ is the adjacency matrix. As an example of potential p_0, we consider that $p_0(v_0) = 1$ in one vertex v_0, and $p_0(v) = 0$ in the other ones, $v \neq v_0$. The application of A to that potential, Ap_0, transfers the value 1 to the vertices adjacent to v_0. That is, $p_1 = Ap_0$ takes the value 1 in vertexes adjacent to v_0, and 0 in others. A second application $p_2 = A^2 p_0$ widens the circle of influence: $p_2(v)$ is the number of paths of two edges from v_0 to v. The iterated application $p_k = A^k p_0$ produces a sequence $p_0, p_1, p_2, \ldots$, in a transfer process. We can assign to the sum of potential $\sum_{i=0}^{n} p_k(v_i)$ the meaning of the total amount of material that comprises p_k. In the process induced by A the total amount of material is not constant, but is multiplied by four in the majority of the vertices, the inner vertices. Therefore is not exactly a diffusion process. Taking another weight on edges, being $w(u,v)$ the inverse of the number of arrows that come out of u, it can be seen that $\sum_{i=0}^{n} p_k(v_i)$ (with $p_k = A_w^k p_0$) is constant, and the process is properly a diffusion process.

It is pertinent to mention iterations in the above example because the eigenvalues p are those potentials that verify $Ap = \lambda p$ (equivalently $A^n p = \lambda^n p$). And they are precisely the potentials invariant (except for a factor λ^n) under iterations of A.

2.4.2 Laplacian and Partitions

A *partition of a set* V is an array (V_1, V_2) of two subsets of V such that

$$V_1 \cup V_2 = V \text{ and } V_1 \cap V_2 = \emptyset.$$

A *partition of a graph* $G = (V,E)$ is a partition of the underlying set of vertices. An edge $u \sim v$ in G is *cut by a partition* (V_1, V_2) if $u \in V_1$ and $v \in V_2$ or vice versa ($u \in V_2$

and $v \in V_1$). If the graph is weighted, the *total weight of the cut*, or total cut, is $\mathrm{cut}(V_1,V_2) = \sum_{\substack{u \in V_1 \\ v \in V_2}} w(u,v)$.

If there are several partitions in a graph, usually is preferable that which minimum number of cuts (or total cut, if weighted). We are interested in partitions with minimal cut, but with balanced number of vertices, that is $\mid V_1 \mid = \mid V_2 \mid$ (if $\mid V \mid$ is even, $\mid V_1 \mid = \mid V_2 \mid \pm 1$ if it is odd). We express the combinatorial problem of finding these partitions using Linear Algebra, in particular the spectrum (that is, eigenvalues and eigenvectors[18]) of the Laplacian matrix, later defined.

Let us suppose given an order $V = \{v_1, v_2, \dots, v_n\}$ in the set of vertices. A vector $x = (x_1, \dots, x_n)$ corresponding to a potential of $\mathbb{R}^V$ has an entry x_i for each v_i. The *characteristic vector* c_S of a set $S \in V$ is $c_S = (c_1, \dots, c_n)$ with:

$$c_i = \begin{cases} 1 \text{ if } v_i \in S \\ 0 \text{ if } v_i \notin S \end{cases}$$

Sometimes is preferable to use other values than 0 or 1 in the vector expression of a combinatorial object like a subset or partition [119]. For two real values b_1, b_2, the (b_1,b_2)*-indicator vector* of a partition (V_1,V_2) is the vector $(x_1, \dots, x_n)$ with

$$x_i = \begin{cases} b_1 \text{ if } v_i \in V_1 \\ b_2 \text{ if } v_i \in V_2 \end{cases}$$

For example, the (0,1)-indicator is the characteristic of the second set of the partition. We use mainly (1,-1)-indicators.

The following proposition summarizes some graph and combinatorial properties expressed in Linear Algebra language. We denote with a dot $\cdot$ the inner product in $\mathbb{R}^V$, and with $\mathbf{1} = (1, \dots, 1)$ the vector all whose entries are 1. The *degree* of a vertex $u \in V$ is the cardinal of the set $\{v \in V$ such that $u \sim v\}$, that is, the number of vertices adjacent to u. The *degree vector* is $(d_1, d_2, \dots, d_n)$ where d_i is the degree of v_i.

Proposition 1. *Let $G = (V,E)$ a graph of adjacency matrix A. For two sets $S,T \subset V$ of characteristics c_S, c_T:*

1. *$\mathbf{1} \cdot c_S$ is the cardinal of S, that is, $\mathbf{1} \cdot c_S = \mid S \mid$. Also $c_S \cdot c_S = \mid S \mid$.*
2. *$c_S \cdot c_T = \mid S \cap T \mid$.*
3. *The vector $A\mathbf{1}$ has, in the i-th entry, the degree of v_i, that is, $A\mathbf{1}$ is the degree vector*
$$A\mathbf{1} = (d_1, d_2, \dots, d_n).$$
Also $\mathbf{1} \cdot A\mathbf{1} = \sum_i d_i$.
4. *Ac_S has, in entry i-th, the number of edges to v_i from a vertex in S. That is, calling $S \sim v = \{s \in V$ such that $s \sim v_{\,and}\, s \in S\}$,*
$$Ac_S = (x_1, x_2, \dots, x_n) \textit{ with } x_i = \mid S \sim v_i \mid$$

[18]We recall, that, given a matrix A, λ is an eigenvalue of A if there exist an vector v such that $Av = \lambda v$. In this case, v is the associated eigenvector of λ.

If A_w is a weighted adjacency matrix, the i-th entry of $A_w c_S$ is the sum of the weight of the edges of the form $s \sim v_i$ with $s \in S$. That is,

$$A_w c_S = (x_1, x_2, \ldots, x_n) \text{ with } x_i = \sum_{u \in S \sim v_i} w(u)$$

Proof. It is easy to do the computations for these claims from the definitions. For example, for c), we have that the i-th entry of $A\mathbf{1}$ is $\sum_{j=0} n a_{ij} \cdot 1$. As a_{ij} is 1 if $v_i \sim v_j$ (and 0 in other case), then $\sum_{j=0}^{n} a_{ij} = \sum_{j|v_i \sim v_j} 1$, that is precisely the number of vertices adjacent to v_i. □ □

If we call D_g the matrix with the degree vector in the diagonal and zero off-diagonal:

$$D_g = \begin{pmatrix} d_1 & 0 & \cdots & 0 \\ 0 & d_2 & & 0 \\ \vdots & & \ddots & \vdots \\ 0 & 0 & \cdots & d_n \end{pmatrix}$$

from a similar easy computation we have $\mathbf{1} \cdot D_g \mathbf{1} = \sum_i d_i$. For any partition, if x is it (1,-1)-indicator, we also have $x \cdot D_g x = \sum_i d_i$, because the minus signs compensate in the entries where them appear.

In this context, it is traditional to define the Laplacian matrix L as

$$L = D_g - A.$$

See for example [121] or [122]. The rationale behind this definition is the following relationship between the cut of a partition and the transform by L of its characteristic vectors.

Theorem 1. *For a partition (V_1, V_2), of (1,-1)-indicator x, we have;*

$$cut(V_1, V_2) = \frac{x \cdot Lx}{4}$$

Proof. For a partition (V_1, V_2), being c_1 and c_2 characteristic vectors of its sets, the sum of the weight of the edges $u \sim v$ with $u \in V_1$ and $v \in V_2$ is $c_1 \cdot Ac_2$. Therefore, $\text{cut}(V_1, V_2) = c_1 \cdot Ac_2$. By the symmetry of A, it is also equal to $c_2 \cdot Ac_1$.

If x is the (1,-1)-indicator of (V_1, V_2), then $x = c_1 - c_2$, and:

$$\begin{aligned} x \cdot Ax &= (c_1 - c_2) \cdot A(c_1 - c_2) = \\ &= c_1 \cdot Ac_1 + c_2 \cdot Ac_2 - (c_1 \cdot Ac_2 + c_2 \cdot Ac_1) = \\ &= c_1 \cdot Ac_1 + c_2 \cdot Ac_2 - 2\text{cut}(V_1, V_2) \end{aligned}$$

Besides, as $c_1 + c_2 = \mathbf{1}$, that is $c_1 = \mathbf{1} - c_2$, then $c_1 \cdot Ac_1 = c_1 \cdot A(\mathbf{1} - c_2) = c_1 \cdot A\mathbf{1} - c_1 \cdot Ac_2$. Likewise $c_2 \cdot Ac_2 = c_2 \cdot A\mathbf{1} - c_2 \cdot Ac_1$, hence

$$\begin{aligned} c_1 \cdot Ac_1 + c_2 \cdot Ac_2 &= c_1 \cdot A\mathbf{1} - c_1 \cdot Ac_2 + c_2 \cdot A\mathbf{1} - c_2 \cdot Ac_1 = \\ &= (c_1 + c_2) \cdot A\mathbf{1} - (c_1 \cdot Ac_2 + c_1 \cdot Ac_2) = \mathbf{1} \cdot A\mathbf{1} - 2\text{cut}(V_1, V_2) \end{aligned}$$

Hence

$$x \cdot Ax = c_1 \cdot Ac_1 + c_2 \cdot Ac_2 - 2\mathrm{cut}(V_1,V_2) =$$
$$= \mathbf{1} \cdot A\mathbf{1} - 2\mathrm{cut}(V_1,V_2) - 2\mathrm{cut}(V_1,V_2) = \sum_i d_i - 4\mathrm{cut}(V_1,V_2)$$

That is, $4\mathrm{cut}(V_1,V_2) = \sum_i d_i - x \cdot Ax$. As $\sum_i d_i = x \cdot D_g x$, we can express $\sum_i d_i - x \cdot Ax = x \cdot D_g x - x \cdot Ax = x \cdot Lx$. Therefore

$$\mathrm{cut}(V_1,V_2) = \frac{x \cdot Lx}{4}$$

□ □

We have deduced this well known identity in matrix form, instead of summatory form as usual, to avoid the index chasing. This way also makes explicit the role of the values b_1, b_2 using in indicators (as it is done in [119]). For example if x is a $(\frac{1}{2}, -\frac{1}{2})$-indicator of (V_1,V_2), then $\mathrm{cut}(V_1,V_2) = x \cdot Lx$. In general if x is a (b_1,b_2)-indicator the cost of its cut is $\frac{x \cdot Lx}{(b_2-b_1)^2}$. This deduction also shows the role of the diagonal degree matrix.

In addition to the expression of cost as a bilineal form with matrix L, we express the requirement that the partition (V_1,V_2) be balanced as $\mathbf{1} \cdot x = 0$. Hence, the problem of finding the balanced partition of minimal cost is the following problem of combinatorial optimization:

$$\begin{array}{ll} \underset{x}{\text{Minimize}} & x \cdot Lx \\ \text{subject to} & x_i = \pm 1,\ i = 1, \ldots, n \\ & \mathbf{1} \cdot x = 0. \end{array}$$

To solve this combinatorial problem it is customary to relax the restrain $x_i = \pm 1$. The relaxed problem has several features that ease its numerical resolution: L is symmetric, hence its eigenvalues are real and there are a orthonormal basis of eigenvectors [123]. Besides, $\mathbf{1}$ is a eigenvector of eigenvalue 0, because $D_g\mathbf{1} - A\mathbf{1} = 0$. Also, the eigenvalues are non-negative [124] $0 = \mu_0 \leq \mu_1 \leq \cdots \leq \mu_{n-1}$ (numbering then without multiplicity $0 = \lambda_0 < \lambda_1 < \cdots < \lambda_k$). These features of L are generally deduced from its expression as summatory of squares, that we have avoided. Here we derive them from standard facts of numerical matrix analysis.

The main result in numerical eigenvalue computation is the Min-max Theorem [120]. In our case, this implies $\lambda_1 = \min_{x \neq 0} \frac{x \cdot Lx}{x \cdot x}$, the minimum is reached in a vector x_1 of norm 1, that is eigenvalue for λ_1. As the eigenvectors of different eigenvalues are orthogonal, $\mathbf{1} \cdot x_1 = 0$. That is x_1 is a solution of the relaxed problem.

The first non-null eigenvalue λ_1 is the Fiedler value and its eigenvector x_1 is the Fiedler vector, by [125]. It solves the relaxed problem, numerically with computational complexity of $O(n^3)$. Rounding x_i gives a $(1,-1)$-indicator of a partition. The solution of the relaxed problem is an approximation of the combinatorial problem. This problem is NP-hard [118], hence the interest of a relaxed approximation. A bound of the error of this approximation, involving λ_1, is given by the bound of Mohar

[126]. Being Δ_g the maximum vertex degree of G, $\Phi(G)$ the cost of the minimal cut, and $Sp(G)$ the cut obtained by Fiedler eigenvector:

$$\Phi(G) \leq Sp(G) \leq \sqrt{\lambda_1(2\Delta_g - \lambda_1)}.$$

These properties, included the bound of Mohar, can be translated for Laplacians with vertex potential, a generalization of the Laplacian that we define in the next subsubsection, and that allows us to extend the spectral partition to unequal vertex load.

2.4.3 Laplacian with Potential of Vertex Weights

A *potential* is a function $p : V \longrightarrow \mathbb{R}$, and its diagonal form is the matrix $D_p = (d_{ij})$ with $d_{ii} = p(x_i)$, $d_{ij} = 0$ if $i \neq j$. The *Laplacian with potential p* (or p-Laplacian) is:

$$L_p = L + D_p$$

That is $L_p = D_g - A + D_p$. Some properties of the p-Laplacian are similar to those of the Laplacian.

If the potential p is non-negative, L_p has a real eigenvalue that is positive and of maximum absolute value between the eigenvalues (known as *Perron eigenvalue*). There is an eigenvector of the Perron eigenvalue that is positive (the *Perron* eigenvector ρ).

The max-min theorem for the operator L_p gives us that $\lambda_1 = \min_{\substack{x \neq 0 \\ x \cdot \rho = 0}} \frac{x \cdot L_p x}{x \cdot x}$, and the minimum is reached in its eigenvectors. Conventionally, the eigenvector of λ_1 of norm 1 and with greater number of nonnegative values is the *Fiedler* vector ϕ.

The spectral decomposition of L_p assure that $\phi \cdot \rho = 0$. This can be viewed, like in the previous Laplacian, that the positive and negative values of the Fiedler vector is an indicator of two sets of vertices that cut V in two parts of equal sum of Perron values.

To build potential p in such a way that the Perron vector ρ have predetermined values ρ_i, we have developed the following result. $A = (a_{ij})$ is the adjacency matrix and $(A\rho)_i$ the i-th component of the vector $A\rho$.

Theorem 2. *The potential*

$$p(x_i) = 1 + a_{ii} - \frac{(A\rho)_i}{\rho_i}$$

has ρ as Perron vector.

By the above discussion, the p-Laplacian of this potential has a Fiedler vector orthogonal to the Perron vector (that is, it produces a partition in parts of equal total load at the vertices), and that in addition, by the extremal Max-min property, minimizes the cost of communications in the relaxed problem.

Also, by taking this Fiedler vector as an approximation to the combinatorial solution, that is, the unrelaxed problem, the error can be bounded with an expression

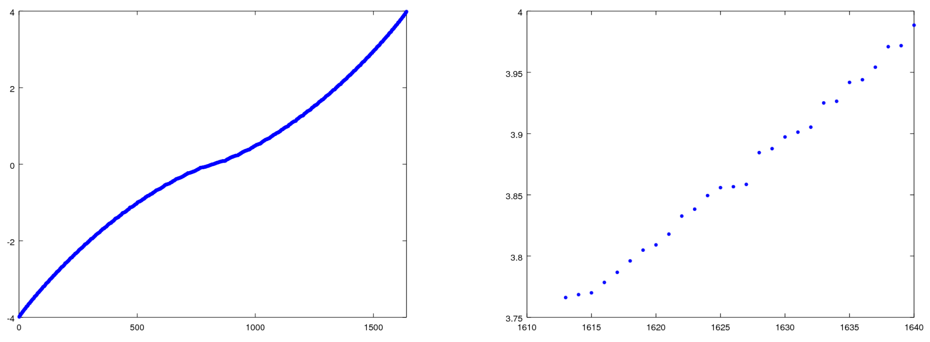

Figure 2.16: Eigenvalues of the mesh. The area of main eigenvalues is zoomed.

similar to that of Mohar. Being, as above, $\Phi(G)$ the cost of the minimal cut, and $Sp_p(G)$ the cut obtained by Fiedler eigenvector of L_p:

$$\Phi(G) \leq Sp_p(G) \leq \sqrt{2\lambda_1 \max_i \frac{d_i - a_{ii}}{\rho_i}}$$

With these results, we can mimic the traditional partition techniques, but incorporating the load at the vertices. In addition, the division into two parts can be done by assigning unequal proportions of the load (for example 30%-70%).

The unequal load has been addressed in the literature either by modeling as a generalized eigenvalue problem [127], or by using several eigenvectors [128]. Both approaches have their own drawbacks [118]. For our purposes, the main disadvantage is that the vertex load is not embodied in the Laplacian. As we want to consider mappings from application graph to machine graph, the loads should be included in the model.

2.4.4 Mesh graph

In this subsection first we give an example of spectral decomposition of the mesh graph of figure 2.15 . We will see that the eigenvector of the dominant eigenvalue partitions the square. In this example of Cartesian graph, the adjacency matrix has side $40 \cdot 41 = 1640$. The 1640 eigenvalues, in increasing order, are plotted in figure 2.16 and, as the matrix is symmetric, the Jordan form is diagonal. [129].

Each vector is a value in every vertex, so we can plot it as a z value of height above the xy plane were the square lattice is displayed. With this convention, the first and second eigenvectors (with respect the ordering eigenvalues) can be seen in figure 2.17.

Note that these are the eigenvectors of the adjacency matrix, not the Laplacian. However, the first eigenvector, bell-shaped and positive, is symmetrically posed in the square. We consider that each vertex has a load proportional to the corresponding entry of this first eigenvector. The second eigenvector, orthogonal to it, has positive and negative entries defining a partition of the mesh, whose two parts are equal in total load (measured by the first eigenvector).

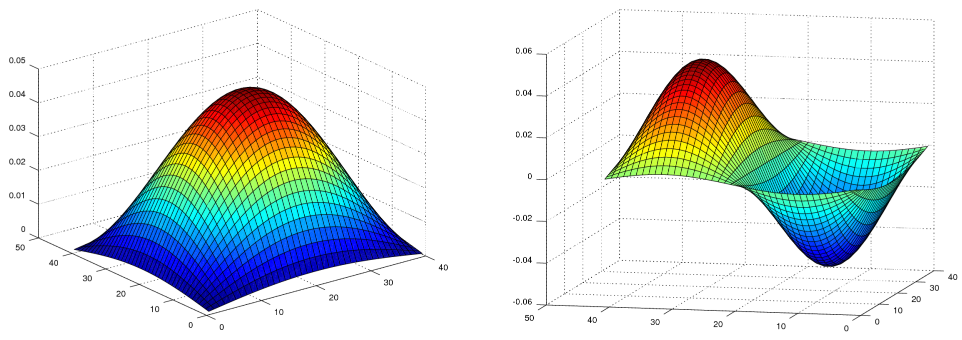

Figure 2.17: The first two eigenvectors of the mesh.

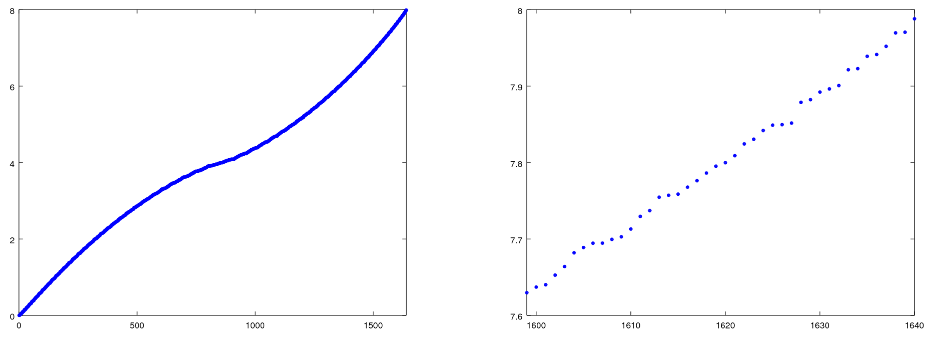

Figure 2.18: Laplacian eigenvalues of square lattice. The area of main eigenvalues is zoomed.

In the case of the Laplacian, first and second eigenvectors (Perron and Fiedler) are in figure 2.18. And these are also, as in the adjacency matrix, one positive and the other partitioning the vertices in two sets of vertices. The sets have equal load, measured by the first eigenvector, that being constant gives us equal number of vertexes in each part.

The adjacency matrix and the Laplacian matrix have been taken as examples. They differ only in the diagonal, so the adjacency matrix is a particular type of *p*-

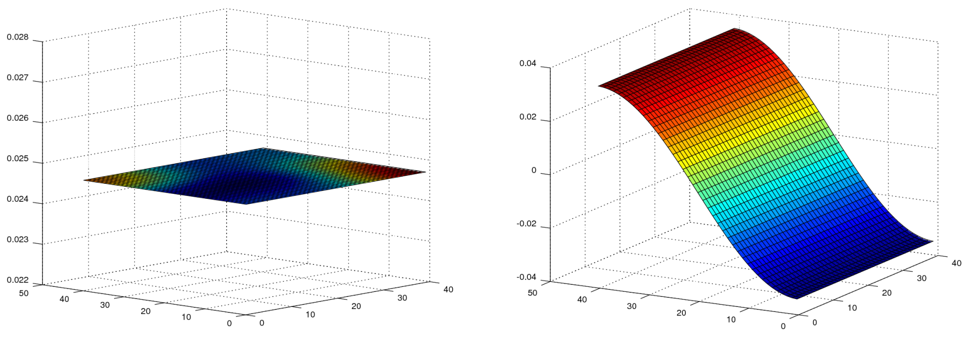

Figure 2.19: Eigenvectors of square lattice.

Laplacian: one that has as potential the degree at each vertex. This example has been considered because it is easy to represent the eigenvectors, and to see that the first eigenvector (Perron in the case of the adjacency matrix) corresponds to a load at each vertex (uniform in the case of Laplacian).

2.4.5 Numerical Experiment

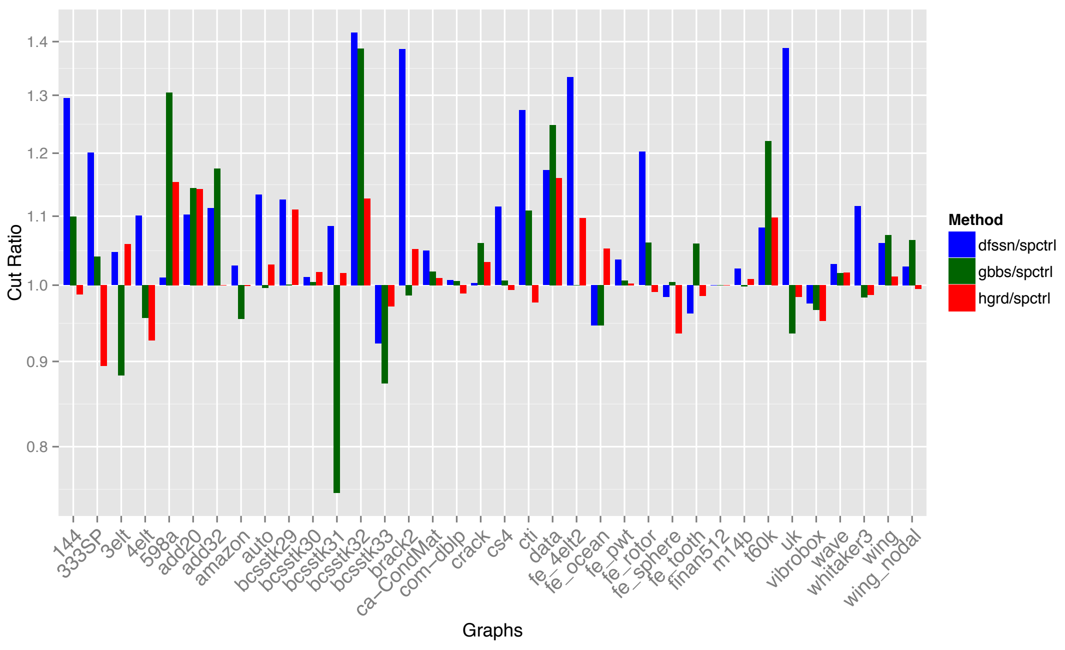

Figure 2.20: Ratio of cut improvement of the spectral method against others.

In this subsection we describe a comparison, using the partitioning software Scotch [130], of the spectral method described above against other method of graph partition. We have integrated the spectral bipartition method (with vertex loads) in Scotch. We resorted to the LAPACK library [131] for the eigenvector computation due to their availability, but it is preferable to use libraries specialized in sparse matrices, such as [132]. The Fiedler eigenvector is used as an initial method in a multilevel approach (see [118] for technical background). In Fig 2.20, we do a comparison with some of the initial methods present in Scotch (Diffusion, Gibbs-Pole-Stockmeyer, H-greedy) over the graphs of the Walshaw collection [133], and also some bigger graphs from the dataset of [134]. The cut produced with the spectral method, for bipartitions, is about 10% better than the other methods. There are some cases where the spectral method behaves equal or worse. In the figure, we plot the value "cost of the cut of other method / cost of the spectral cut ", hence a value of 1 means equal cost, greater than 1 means that spectral has lower cost.

The tests are meant to compare initial methods, leaving the contribution of coarsening-uncoarsening as equal as possible between methods. To be precise, the tests include, for each graph of Walshaw benchmark (excluding fe_body and MemPlus, which are not connected) five different coarsening processes: up to 64, or 128, or 256, or 512, or 1024 vertices. Then each of these initial graph is bipartitioned by

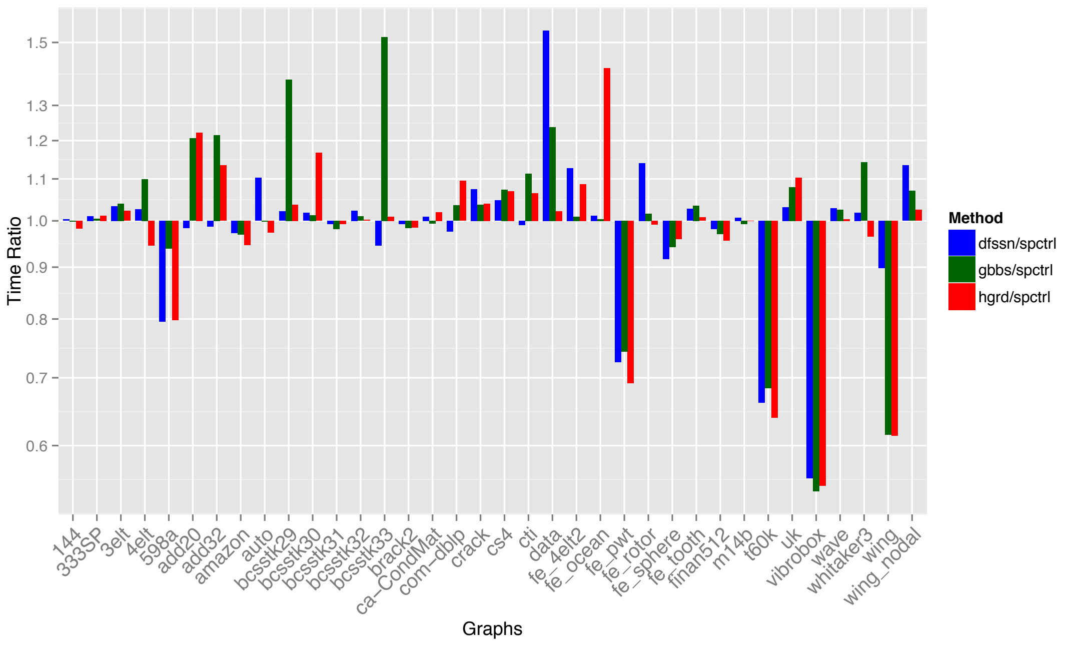

Figure 2.21: Ratio of time improvement of the spectral method against others

diffusion, Gibbs, hgreedy and spectral methods, and then are uncoarsened with the Fiduccia-Mattheyses algorithm [135]. The final measure is the cost of the cut obtained. Unit loads and weights of the input graph are considered. In the plot we use the mean of the five measures for each pair graph-method.

In Figure 2.21 we also compare the timing of running each method compared to the spectral method. We plot the ratio of the time of three other ones compared to the spectral method (hence the higher, the faster the spectral method). We see balanced results here where in some cases the spectral method is much faster but for some graphs (e.g. vibrobox) the ratio is lower than 0.6. However, the geometric mean of the ratio is 0.986, which means that, on average, the spectral method is comparable in terms of timings to the other methods. This is a good result as computing the eigenvectors can be very long. Actually, the coarsening phase that happens only in the other methods takes also a lot of time that has a strong impact on the timings.

2.4.6 *Conclusions*

The bipartition through the Fiedler eigenvector can be done by incorporating the loads of the vertices in the model of the graph, without the need to introduce these loads a posteriori in the resolution process. The classical techniques of analysis of the error of the approximation can be generalized to this new approach. Bipartition can be done in unbalanced parts, with a predetermined ratio, minimizing communications. However, extending this scheme to partitions in three or more parts does not seem straightforward. The numerical results, in comparison with the more usual methods, are favorable to the spectral method, especially in graphs of a certain type, such as those from social networks.

2.5 Summary

This paper has shown some works related to UCS and the variety of systems that cloud be integrated in those complex environments. However, there are still several research topics and challenges that must be faced to cope with such complexity. Below, some of them are shown

Cloud/Fog/Dew Big Data Computing: In the future the highest opportunities lie in the availability of massive scale cloud infrastructure which will be omnipresent. To effectively use these available resources, massively federated and scalable software with orchestration through network awareness will be necessary. As an extension of links between UCS and Clouds, data access models for data mining in Exascale systems will be a key research topic. The integration will be between Cloud systems but also Fog and future type of infrastructure, leading to need on machine-to-machine computing and Cloud computing integration. Heterogeneity of such system will continue to increase, leading to the need to be able to integrate warehouse-scale computing using purpose-designed chips. Integrating the lowest, Dew-level devices will present additional challanges due to the extreme quantities of Physical Edge Devices, their severely low processing power and communication means, and the huge amounts of data generated.

HPC: One of the key point will be the availability of programming abstractions for the different fields of Exascale such as data analysis, machine learning, scientific computing, Big Data management, smart cities, that will be based on asynchronous algorithms for overlapping communication and computation. To reach this overlap, parallel applications (such as the MPI-based one) will need to be optimized using platform topology and performance information. One crucial research topic will be programmability of UCS as applications will run millions of parallel execution flows. New workflow programming for very large plate forms will be needed. But interoperability and sustainability will only be reached when code will be prevented to be platform specific and still efficient on different platforms. From a broader point of view, the scale of UCS will lead to Supercomputing on demand leading to a better use of the vast amount of available resources. The efficiency will be linked to researches on performance evaluation, modelling and optimization of data parallel applications on heterogeneous HPC platforms. Management of such large distributed systems will be based on future researches on complex systems modelling, self-organizing systems and cellular automata.

Application-driven topics: With the aim of harnessing the power of UCS, scientific community will be able to improve dramatically the quality of models. One key example will be the research focus on meteorology beyond wind simulation (Interfacing between different software packages and data formats, necessary for integration of simulations for complex tasks). New tools will be needed to use UCS for scientists from diverse fields, but tools only available to computer scientists will be needed such as the Hardware/Software Co-design models to guide together the development of hardware and software infrastructure.

Tool-driven: Several tools will be needed to use efficiently UCS. Some tools can be provided by software, but also abstract models and new programming paradigms helping programmers to better use the available resources are helpful. Due to the scale of the systems, one key element will be resource-efficient models for automatic recovery from minute-to-minute failures. As security is often forgotten by programmers, software-defined security models will be needed on large scale distributed infrastructure to simplify its usage. One way to increase security and privacy will be to create new secure Privacy-Preserving data management algorithms such as machine learning. To address code sustainability and adaptation evolution on code production is needed such as source-to-source translators and MDE (Model Driven Engineering) in order to adapt to the underlying hardware.

In order to support some of those challenges, several breaktroughs are expected in order to reach proper support for programmers and users in the Ultrascale context as described in the NESUS research roadmap[6]:

Improve the programmability of complex systems Due to the size of these systems, it is no more possible for the programmer to have a precised and detailed global view of the state of its application. Thus he needs to have support from programming frameworks to simplify this view;

Break the wall between runtime and programming frameworks Exascale sytems are so complex that runtime need high level information from the programmers and the programmer need some information on the runtime to understand how to harness its power;

Enabling behavioral sensitive runtime. Runtime cannot run application as black boxes anymore as large scale systems are composed of a large number of interconnected elements. Network profile must be known to reduce impact on neighboor applications for example.

Chapter 3
RESILIENCE AND FAULT TOLERANCE

Pascal Bouvry[1] and Sebastien Varrette[2] and Tuan Anh Trinh[3] and Muhammad Umer Wasim[4] and Abdallah A.Z.A. Ibrahim[5] and Xavier Besseron [6]

Keywords: resilience, fault tolerance, compliance, AI, blockchain, resource dynamic reallocation, resilience, Ultra-scale.

As discussed in the Introduction, Ultrascale computing is a new computing paradigm that comes naturally from the necessity of computing systems that should be able to handle massive data in possibly very large scale distributed systems, enabling new forms of applications that can serve a very large amount of users and in a timely manner that we have never experienced before. It is very challenging to find sustainable solutions for UCS due to their scale and a wide range of possible applications and involved technologies. For example, we need to deal with cross fertilization among HPC, large scale distributed systems, and big data management.

One of the challenges regarding sustainable UCS is resilience. Traditionally, it has been an important aspect in the area of critical infrastructure protection (e.g. the traditional electrical grid and the smart grids). Furthermore, it has also become popular in the area of information and communication technology (ICT), ICT systems, computing and large-scale distributed systems. The existing practices of dependable design deal reasonably well with achieving and predicting dependability in systems that are relatively closed and unchanging. Yet, the tendency to make all kinds of large-scale systems more interconnected, open, and able to change without new intervention by designers, makes existing techniques inadequate to deliver the same levels of dependability. For instance, evolution of the system itself and its uses impairs dependability: new components "create" system design faults or vulnerabilities by feature interaction or by triggering pre-existing bugs in existing components; likewise,

[1]University of Luxembourg,Luxembourg
[2]University of Luxembourg, Luxembourg
[3]Corvinus University of Budapest, Hungary
[4]University of Luxembourg, Luxembourg
[5]University of Luxembourg, Luxembourg
[6]University of Luxembourg, Luxembourg

new patterns of use arise, new interconnections open the system to attack by new potential adversaries, and so on. Another one, which attracted less interest in the literature, but becomes more and more crucial with the expected convergence with the Cloud computing paradigm, is the notion of regulation in such system to assess the QoS and SLA proposed for the use of these platforms. This chapter covers both aspects through the reproduction of two articles: [3] and [136].

In this chapter, we show an introduction to resilience in UCS form two facets: technical and legal. Thus, the rest of this chapter is organized as follows: Section 3.1 reviews the basic notions of faults, fault tolerance and robustness. Applications and implementations within UCS are also proposed, while novel challenges and opportunities linked to the development of DLT. Then regulation compliance aspects are covered in the section 3.2. Finally, Section 3.3 concludes the paper and provides some future directions and perspectives opened by this study.

3.1 Security and reliability in Ultra-scale System

3.1.1 Faults, Fault Tolerance and Robustness

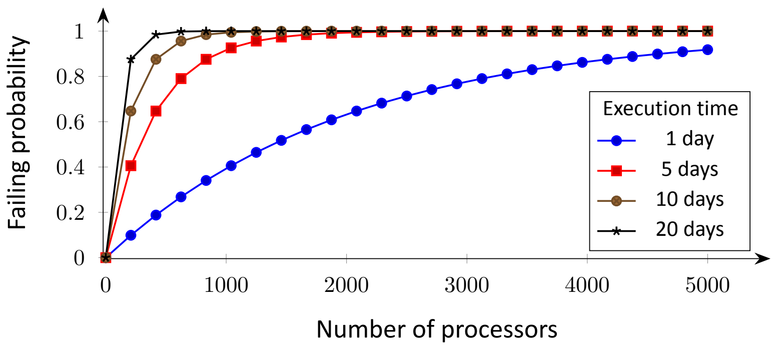

Figure 3.1: Typical probability of failure with increasing number of processors in a computing system.

As as illustrated in the Figure 3.1 and due to their inherent scale, UCS are naturally prone to errors and failures which are no longer rare events [137, 138, 139, 140].

There are many sources of *faults* in distributed computing and they are inevitable due to the defects introduced into the system at the stages of its design, construction or through its exploitation (e.g. software bugs, hardware faults, problems with data transfer) [141, 138, 139, 140]. A fault may occur by a deviation of a system from the required operation leading to an *error* (for instance a software bug becomes apparent after a subroutine call). This transition is called a fault activation, *i.e.* a *dormant* fault (not producing any errors) becomes *active*. An error is *detected* if its presence is indicated by a message or a signal, whereas not detected, present errors are called *latent*. Errors in the system may cause a (service) *failure* and depending on its type, successive faults and errors may be introduced (*error/failure propagation*). The distinction between faults, errors and failures is important because these terms create boundaries allowing analysis and coping with different threats. In essence, faults are the cause of errors (reflected in the state) which without proper handling may lead to failures (wrong and unexpected outcome). Following these definitions, *fault tolerance* is an ability of a system to behave in a well-defined manner once an error occurs.

There are five specific fault models relevant in distributed computing: *omission*, *duplication*, *timing*, *crash*, and *byzantine failures* [141, **?**].

Omission and *duplication* failures are linked with problems in communication. Send-omission corresponds to a situation, when a message is not sent; receive-omission — when a message is not received. Duplication failures occur in the opposite situation — a message is sent or received more than once.

Timing failures occur when time constraints concerning the service execution or data delivery are not met. This type is not limited to delays only, since too early delivery of a service may also be undesirable.

The *crash* failure occurs in four variants, each additionally associated with its persistence. Transient crash failures correspond to the service restart: amnesia-crash (the system is restored to a predefined initial state, independent on the previous inputs), partial-amnesia-crash (a part of the system stays in the state before the crash, where the rest is reset to the initial conditions), and pause-crash (the system is restored to the state it had before the crash). Halt-crash is a permanent failure encountered when the system or the service is not restarted and remains unresponsive.

The last model — *byzantine* failure (also called *arbitrary*) — covers any (very often unexpected and inconsistent) responses of a service or a system at arbitrary times. In this case, failures may emerge periodically with varying results, scope, effects, etc. This is the most general and serious type of failure [141, **?**].

Dependable computing and Fault tolerance techniques

Faults, errors and failures are *threats* to system's *dependability*. A system is described as dependable, when it is able to fulfil a contract for the delivery of its services avoiding frequent downtimes caused by failures.

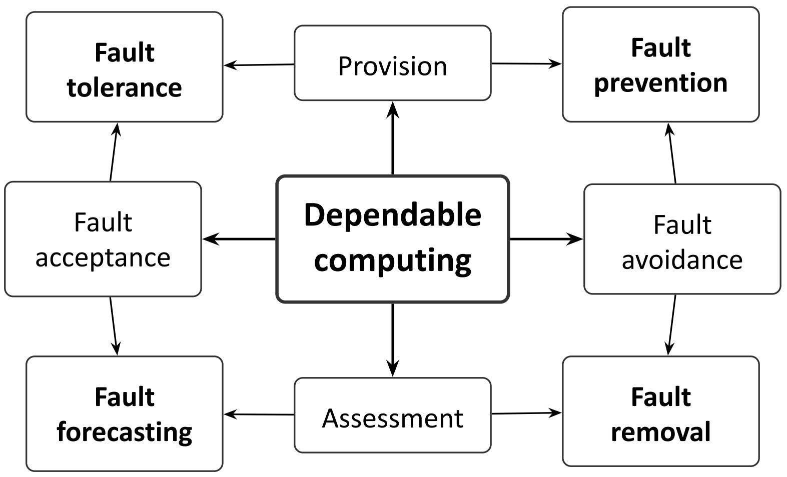

Figure 3.2: Means for dependable computing [3]

Identification of threats does not automatically guarantee dependable computing. For this purpose, four main groups of appropriate methods have been defined [141]:

fault prevention, *fault tolerance*, *fault removal*, and *fault forecasting*. As visible on fig. 3.2, all of them can be analyzed from two points of view — either as means of avoidance/acceptance of faults or as approaches to support/assess dependability. Fault tolerance techniques aim to reduce (or even eliminate) the amount of service failures in the presence of faults. The main goal of *fault prevention* methods is to minimize the number of faults occurred or introduced through usage and enforcement of various policies (concerning usage, access, development etc.) The next group — *fault removal* techniques — is concentrated around testing and verification (including formal methods). Finally, *fault forecasting* consists of means to estimate occurrences and consequences of faults (at a given time and later).

Fault tolerance techniques may be divided into two main and complementary categories [141]: *error detection*, and *recovery*. Error detection may be performed during normal service operation or while it is suspended. The first approach in this category — *concurrent detection* — is based on various tests carried out by components (software and/or hardware) involved in the particular activity or by elements specially designated for this function. For example, a component may calculate and verify checksums for the data which is processed by it. On the other hand, a firewall is a good illustration of a designated piece of hardware (or software) oriented on detection of intrusions and other malicious activities. *Preemptive detection* is associated with the maintenance and diagnostics of a system or a service. The focus in this approach is laid on identification of latent faults and dormant errors. It may be carried out at a system startup, at a service bootstrap, or during special maintenance sessions. After an error of a fault is detected, recovery methods are applied. Depending on the problem type, *error or fault handling* techniques are used. The first group is focused on elimination of errors from the system state, while the second are designed to prevent activation of faults. In [141], the specific methods are separated from each other, where in practice this boundary is fuzzy and depends on the specific service and system types. Generally, error handling is solved through:

1. *Rollback* [142]: the system is restored to the last known, error-free state. The approach here depends on a method used to track the changes of the state. A well known technique is *checkpointing* — the state of a system is saved periodically (e.g. the snapshot of a process is stored on a disk) as a potential recovery point in the future. Obviously, this solution is not straightforward in the case of distributed systems and there are many factors to consider. In such environment, checkpointing can be coordinated or not — with differences in reliability and the cost of synchronisation of the distributed components – see [**?**, **?**, **?**].
   Rollback can be also implemented through the *message logging*. In this case, the communication between the components is tracked rather than their state. In case of an error, the system is restored by *replaying* the historical messages, allowing it to reach global consistency [**?**]. Sometimes both techniques are treated as one, as usually they complement each other.
2. *Rollforward*: the current, erroneous system state is discarded and replaced with a one newly created and initialised.

3. *Compensation*, an approach based on components' *redundancy* and *replication*, sometimes referred to as *fault masking*. In the first case, additional components (usually hardware) are kept in reserve [?]. If failures or errors occur, they are used to compensate the losses. For example, a connection to the Internet of a cloud platform should be based on solutions from at least two different ISP.

   Replication is based on the dispersion of multiple copies of the service components. A schema with replicas used only for the purpose of fault tolerance is called a *passive (primary-backup) replication* [?]. On the other hand, an *active replication* is when the replicas participate in providing the service, leading to increased performance and applicability of load balancing techniques. Coherence is the major challenge here, and various approaches are used to support it. For instance, read-write protocols are crucial in active replication, as all replicas are expected to have the same state. Another worth to note example is clearly visible in volunteer-based platforms. An appropriate selection policy of the correct service response is needed when replicas return different answers, *i.e.* a method to reach quorum consensus is required.

These techniques are not exclusive and can be used together. If the system can not be restored to a correct state thanks to the compensation, rollback may be attempted. If this fails, then rollforward may be used.
The above methods may be referred to as *general-purpose* techniques. These solutions are relatively generic, which aids their implementation for almost any distributed computation. It is also possible to delegate responsibility for fault tolerance to the service (or application) itself, allowing tailoring the solution for specific needs — therefore forming an *application-specific* approach. A perfect example in this context is ABFT, originally applied to distributed matrix operations [143], where original matrices are extended with checksums before being scattered among the processing resources. This allows detection, location and correction of certain miscalculations, creating a *disk-less checkpointing* method. Similarly, in certain cases it is possible to continue the computation or the service operation despite the occurring errors. For instance, unavailable resource resulting from a crash-stop failure can be excluded from further use. In this work, the idea will be further analysed and extended to the context of byzantine errors and the nature-inspired distributed algorithms.

Fault handling techniques are applied after the system is restored to an error-free state (using the methods described above). As the aim now is to prevent future activation of detected faults, four subgroups according to the intention of the operation may be created. These are [141]: *diagnosis* (the error(s) are identified and their source(s) are located), *isolation* (faulty components are logically or physically separated and excluded from the service), *reconfiguration* (the service/platform is reconfigured to substitute or bypass the faulty elements), and *reinitialization* (the configuration of the system is adapted to the new conditions).

Robustness

When a given system is resilient to a given type of fault, one generally claims that this system is *robust*. Yet defining rigorously robustness is not an easy task and many contributions come with their own interpretation of what robustness is. Actually, there exists a systematic framework that permits to define a robust system unambiguously. In fact, this should be probably applied to any system or approach claiming to propose a fault-tolerance mechanism. This framework, formalized in [144], answers the following three questions:

1. What behavior of the system makes it robust?
2. What uncertainties is the system robust against?
3. Quantitatively, exactly how robust is the system?

The first question is generally linked to the technique or the algorithm applied. The second — explicitly lists the type of faults or disturbing elements targeted by the system. Answering it is critical to delimit the application range of the designed system and to avoid counter examples selected in a context not addressed by the robust mechanism. The third and the last question is probably the most difficult to answer, and at the same time the most vital to characterize the limits of the system. Indeed, there is nearly always a threshold on the error/fault rate above which the proposed infrastructure fails to remain robust and breaks (in some sense).

3.1.2 Fault Tolerance in UCS

Computing Hardware Resilience

As mentioned before, any implementation of fault tolerance (or indeed of fault detection) in hardware implies compensation, *i.e.* the use of *redundancy* and *replication*. In terms of data or information redundancy, a general approach consists in the use of non-minimal coding to represent the data in a system. By far the most common implementation of data redundancy implies the use of *error detecting codes* (EDC), when the objective is fault detection, and of *error correcting codes* (ECC), when the objective is fault tolerance [145].

Memory elements for instance are probably the hardware components that require the highest degree of fault tolerance: their extremely regular structure implies that transistor density in memories is substantially greater than in any other device (the largest memory device commercial available in 2015 reaches a transistor count of almost 140 billion, compared for example to the 4.3 billion of the largest processor). This level of density has resulted in the introduction of fault tolerant features even in commonly available commercial memories. Reliability in memories takes essentially two forms: to protect against single faults, the use of redundant ECC memory is common and well-advertised [146], while marginally less known is the use of spare memory locations to replace permanently damaged ones. The latter technique, used extensively at fabrication for laser-based permanent reconfiguration, has also been applied in an on-line self-repair setting [147].

At the level of the computing elements, the development of high-performance processors has been driven by both performance and energy efficiency. As a result and due to their redundancy requirements and thus their negative implications both for performance and for power consumption, relatively little research into fault tolerant cores has reached the consumer market, leading to limited developments. The situation is somewhat different outside of the high-performance market (typically in the spatial domain), where examples of processors specifically designed for fault tolerance exist.

More recently, the RAZOR approach [148] represents a fault tolerance technique aimed specifically at detecting (and possibly correcting) timing errors within processor pipelines using a particular kind of time redundancy approach that exploits delays in the clock distribution lines.

Network Resilience

Networks are a crucial element of UCS and more generally any system where processors have to share information, and therefore they represent a fundamental aspect of any multi-processor system. Often rivalling in size and complexity with the processing units themselves, networks and their routers have traditionally been a fertile ground for research on fault tolerance. Indeed, even when limiting the scope of the investigation to on-chip networks, numerous books and surveys exist that classify, describe, and analyse the most significant approaches to fault tolerance [149][150][151]). Very broadly, most of the fundamental redundancy techniques have been applied, in one form or another, to the problem of implementing fault-tolerant on-chip networks, ranging from data redundancy (*i.e.* parity or ECC encoding of transmitted packets), through hardware redundancy (*i.e.* additional routing logic), to time redundancy (*i.e.* repeated data transmission).

Recent studies [152] also consider a change in the communication pattern, typically using self-healing protocols based on *gossiping*. Gossip protocols define a pure P2P network over a large set of computing resources and exploit randomness to virally disseminate information while maintaining connectivity in a self-organized (independent of the initial state) equilibrium. Such equilibrium emerges from the loosely-coupled and distributed run of the protocol within different and independent communicating components. The epidemic nature provides high fault-resilience and self-healing properties meant to be crucial for large-scale computing platforms as UCS, at the cost of an overhead in terms of messages routing performance [153].

Software and MPI Resilience

We have mentioned previously that application specific approaches relying on ABFT which permit to tailor the fault-tolerant mechanism solution for specific needs, therefore forming an *application-specific* approach.

More generally, the compute units of current and future HPC systems are more and more complex and diverse (including for instance co-processors or GPU accelerators) such that smarter ways to efficiently program them are required. At this level, programming models initially introduced to abstract from the compute resources and leverage available parallelism, have to adapt. In particular, parallel programming models meant as ways to express parallelism inside applications, have to be compliant with a common programming language, which comes with a compiler and a runtime to ensure an efficient execution.

Various programming models have emerged as parallel machines evolved, and they follow different paradigms, yet the most popular one is based on Message Passing oriented toward distributed and interconnected memory systems. In this model, multiple instances of the program (or processes) allow to share computational resources. A process contains everything needed for executing a program: its own address space, a set of instructions, and a context. They communicate with each other through messages passed over the network.

The main implementation of this model is of course MPI, a standard library introduced in 1991. It is designed for distributed memory machines, and it involves processes running concurrently and parallelizing the program. Communications are to be made explicit by the user and MPI supports both point-to-point as well as collective communications. It is now widely and largely adopted for most scientific codes, having interfaces in many programming languages. The standard has been revised in multiple versions, the most recent being the MPI 3.1 [154] standard which introduced Non Blocking Collectives, allowing asynchronous communications between processes.

Numerous implementations of MPI are available, such as OpenMPI, MPICH2, MVAPICH2, Intel MPI or MPC (Multi-Processor Computing).

Nowadays, MPI remains a straightforward and effective way to program large-scale MPI. Fault tolerance aspects are reviewed in [155] as the MPI standard does not clearly define behavior of MPI implementation if one or several processes of an MPI application are abnormally aborted. There is a dedicated working group[7] covering this topic, and several MPI implementations embed fault tolerance mechanisms. First attempts rely on a complete checkpointing and message logging to enable replacement of aborted processes – the checkpoints avoid reconstructing computations from the beginning through the message logs. This requires a reliable subsystem for the checkpoints and message logs, as well as for the "dispatcher" process leading to a *coordinated* checkpoint. More recent approaches try to mitigate this requirement, such as the one proposed in ULFM 2.0, Intel MPI or MPICH. For instance, ULFM enables user-level deployment of in-memory diskless checkpoints, stored on other compute nodes. It features reduced I/O activities to offer a decreased the failure free overhead while enabling better restart speed. Yet its development remains at an early stage. In all cases, building a resilient MPI program encompasses a minimal set of features:

- *Detection and notification of failures.* Typically only processes involved in a communication with a failed process might detect the occurence of a failure to limit the scope and noise induced by the detection operations.
- *Definition of a failure scope to enable error propagation.* This is typically left to application-specific settings.
- *Error Recovery strategy.* This remains of course the main issue to solve and a work in progress, for instance to define who should be in charge of defining the fault-tolerant strategy and the type of feedback the application receive. As an illustration, at the moment of writing, ULFM is not a recovery strategy, but a minimalistic set of building blocks for implementing complex recovery strategies.

3.1.3 Blockchains and DLT

Blockchains are immutable DLT system implemented in a distributed fashion (*i.e.* without a central repository) and usually without a central authority [156]. At their

[7]See http://mpi-forum.org/mpi-30/ft-wg

most basic level, they enable a community of users to record transactions in a ledger that is public to that community, such that no transaction can be changed once published. This technology became widely known starting in 2008 when it was applied to enable the emergence of electronic currencies where digital transfers of money take place in distributed systems. It has enabled the success of e-commerce systems such as Bitcoin, Ethereum, Ripple, and Litecoin [157]. Because of this, blockchains are often viewed as bound to Bitcoin or possibly e-currency solutions in general. However, the technology is more broadly useful and is available for a variety of applications.

Indeed at the heart of DLT resides a consensus algorithm which is responsible for maintaining the data structure *i.e.* define the way new blocks representing sets of transactions are added. Each node maintains a copy of the blockchain and may propose a new block to the other participating nodes (called miners in the traditional PoW consensus model). Thus the consensus model enable a group of mutually distrusting users to work together to decide which block is agreed to expand the structure, and without any central authority. A list of the main consensus models currently available is proposed in the Table 3.1.

Consensus Model	**Example**
PoA	POANetwork, Kovan and Rinkeby *testnets*...
PoW	Bitcoin, Ethereum (until version 3), Litecoin, Primecoin, Monero, Zcash, Namecoin...
PoS	Peercoin (PoST), Ethereum (starting version 4), Netcoin (PoU)...
DPoS	Nano / Raiblocks (block lattice)...
PoR	Spacemint...
DAG	IOTA (Tangle), Hashgraph...
BFT	PBFT, Ripple (FBA), Algorand (BA $\star$)...

Table 3.1 Overview of the main consensus models used within DLT.

The traditional PoW is not adapted for UCS – it involves intentionally resource-intensive tasks (taking large amounts of processing power, memory, or both) yet using these systems for these duties is counter-productive and against energy efficiency objectives. More recent and alternative proposals seems more suited for an effective usage on UCS, typically the ones relying on PoS, DAG and the resolution of the BGP enabling BFT. The range of possible applications is wide, for instance to securely store computing transactions or to enable QoS regulation from *smart contracts*.
A smart contract is a collection of code and data (sometimes referred to as functions and state) that is deployed to a blockchain such as Ethereum. Any future transactions sent to the blockchain can then send data to public methods offered by the smart contract. The contract executes the appropriate method with the user provided data to perform a service. The code, being on the blockchain, is immutable and therefore can be used (among other purposes) as a trusted third party for validating the SLA of the system. The next section demonstrates such a use case.

3.2 Regulation Compliance in Ultra-scale System

Today's law driven societies based on the use of smart contracts, are transforming the way economies function around the globe.Regulation compliance is the common model used to ensure desired level of reliability in any system, which is expected to be more an more crucial for large-scale computing platforms such as UCS.

Leaving aside the technological details of the running a smart contract on top of such systems, this section presents the design and implementation of NESUS Watchdog, a software bot/agent adapted from the one proposed in [136] and inspired from the work performed in [158]. The underlying concept of NESUS Watchdog is built upon the notion factor analysis and stochastic modeling from the disciplines of unsupervised machine learning and Data Science, respectively. The aim of NESUS Watchdog is to monitor an UCS as per pre-define regulations (a *smart contract*) and penalize the system in case of a breach that (a) has a potential to create substantial damage and (b) has high probability to occur in the future.

3.2.1 NESUS Watchdog and Regulatory Compliance

As seen in the section 3.1.3, a smart contract is a piece of code that resides on a blockchain network and is identified by a unique address. It includes a set of executable functions and state variables. The functions are executed when a transaction is invoked by a certain condition (or by an electronic event or data). These transactions include input parameters that are required by the functions in the contract. Upon the execution of a function, the state variables in the contract may change depending on the logic implemented in the function. This execution is self-enforceable, i.e. once a smart contract is concluded its further execution is neither dependent on intend of contractual parties or any unplanned third part, nor does it require any additional approvals or actions from their side [159]. Thus breach of contract and mechanism addressing the breach becomes irrelevant during the execution of a smart contract [160]. However, even though the breach becomes irrelevant during the execution, what if an output of a smart contract results in a breach? For example, deviation in an output of a smart contract is a breach if a service provider of an UCS provides "90% actual uptime" on average as compared to agreed "95% uptime".

The NESUS Watchdog, hereafter referred as a *bot*, reuse the concepts proposed in [158] and performs a two-phase validation process for the potential breach by a smart contract executed on top of an UCS. Initially, it assesses significance of the breach to ensure that it has a potential to create substantial damage. Afterwards, if the significance is high, it assesses the probability of the breach. In case the probability is also high, i.e. the breach frequently occurred in the past and there is certainty for it to occur in the future, the bot invokes a transaction and executes a function in a smart contract that results in the penalization. Figure 3.3 presents an example of a smart contract for quality of service (QoS) in an UCS and a context where the contract is implemented using the bot.

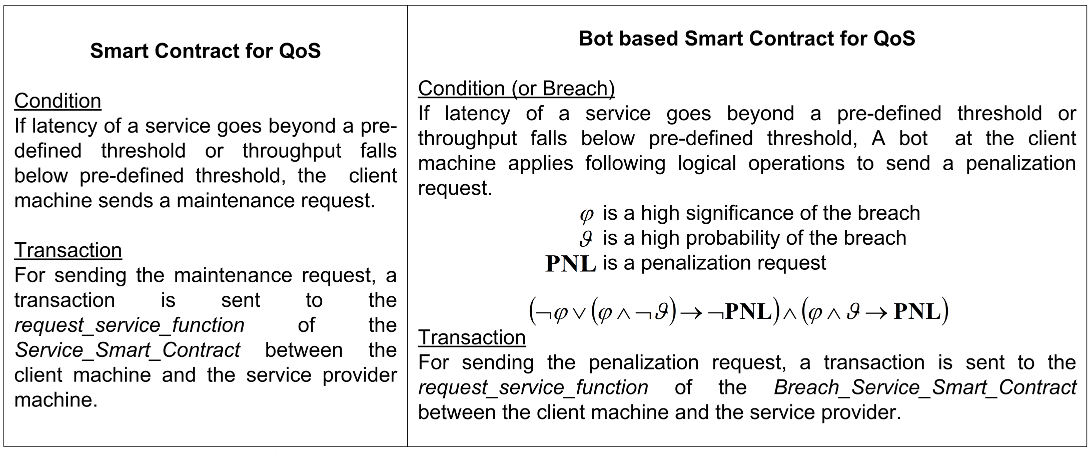

Smart Contract for QoS	**Bot based Smart Contract for QoS**
Condition If latency of a service goes beyond a pre-defined threshold or throughput falls below pre-defined threshold, the client machine sends a maintenance request. Transaction For sending the maintenance request, a transaction is sent to the *request_service_function* of the *Service_Smart_Contract* between the client machine and the service provider machine.	Condition (or Breach) If latency of a service goes beyond a pre-defined threshold or throughput falls below pre-defined threshold, A bot at the client machine applies following logical operations to send a penalization request. φ is a high significance of the breach ϑ is a high probability of the breach $\mathbf{PNL}$ is a penalization request $\left(\neg\varphi \vee (\varphi \wedge \neg\vartheta) \rightarrow \neg\mathbf{PNL}\right) \wedge \left(\varphi \wedge \vartheta \rightarrow \mathbf{PNL}\right)$ Transaction For sending the penalization request, a transaction is sent to the *request_service_function* of the *Breach_Service_Smart_Contract* between the client machine and the service provider.

Figure 3.3: The Bot enabled Smart Contract

Assessing Significance of Breach

To assess the significance of a breach within the system, the bot relies on the notion of *communality* [161], a measure of variance a broader concept of Probability-based Factor Model (PFM) from the discipline of unsupervised machine learning [162] [163]. In the example provided in Figure 3.3, it would correspond to the measure of the relationship between contract (QoS) and its output e.g. latency. Its high value indicates a strong relationship between the two and endorses the related breach, e.g. latency > threshold), to be considered as significant.

Communality is estimated by using SEM. SEM is a statistical approach used to examine association between a *latent* variable (or goal) and an observed variables (or criteria) [162] [163]. Latent variable is a theoretical construct that is inferred from the variables that are observed in the field. In figure 3.3, QoS is a latent variable, which is inferred from the variables (throughput or latency) that are observed during in the field. In SEM, the most popular and frequently used methods to estimate communality are Principal Factor Analysis (PFA) and Maximum Likelihood (ML) [162] [163]. Considering that ML estimation assumes normal distribution of observed variables and that the bot deals with observed variables without making any prior assumption, PFA was used to estimate communality. In PFA, the relationship vector $\Lambda = (\lambda_1 \lambda_2 \ldots \lambda_n)'$ between a latent variable F and observed variables vector $Y = (y_1 y_2 \ldots y_n)'$ is expressed in a variance-covariance matrix notation as:

$$cov(Y) = cov(\Lambda F) + \Psi,$$

where Ψ is a vector that represents uniqueness of observed variables not shared with the latent variable. By using covariance property $cov(AZ) = Acov(Z)A^T$, $cov(\Lambda F)$ in the right hand side of above equation can be expanded to $\Lambda cov(F)\Lambda^T + \Psi$. Moreover, since we consider here only a *single* latent factor (the QoS), F is simply an identity matrix, thus $cov(F) = 1$. It follows that:

$$cov(Y) = \Lambda\Lambda^T + \Psi$$

Within HPC and UCSs, Y is generally not *commensurated*, i.e. observed variables (throughput, latency etc.) are measured in different units and scales. In this case, standardized Y has to be used. After standardization, the covariance becomes correlation (r) and subsequently, the covariance matrix $cov(Y)$ becomes a correlation matrix $R = \Lambda\Lambda^T + \Psi$, which can be expanded as:

$$\begin{bmatrix} 1 & \cdots & r_{1n} \\ \vdots & \ddots & \vdots \\ r_{1n} & \cdots & 1 \end{bmatrix} = \begin{bmatrix} \lambda_1 \\ \lambda_2 \\ \vdots \\ \lambda_n \end{bmatrix} \begin{bmatrix} \lambda_1 & \lambda_2 & \cdots & \lambda_n \end{bmatrix} + \begin{bmatrix} \Psi_1 & \cdots & 0 \\ \vdots & \ddots & \vdots \\ 0 & \cdots & \Psi_n \end{bmatrix}$$

Bringing Ψ to left hand side and performing subtraction,

$$\begin{bmatrix} 1-\Psi_1 & \cdots & r_{1n} \\ \vdots & \ddots & \vdots \\ r_{1n} & \cdots & 1-\Psi_1 \end{bmatrix} = \begin{bmatrix} \lambda_1 \\ \lambda_2 \\ \vdots \\ \lambda_n \end{bmatrix} \begin{bmatrix} \lambda_1 & \lambda_2 & \cdots & \lambda_n \end{bmatrix} = \Lambda\Lambda^T$$

Subtracting unique variance from one $(1-\Psi)$ will yield shared variance of an observed variable for the latent variable, which is equal to square of λ_i [162] [163]. Respectively, $(\lambda_i)^2$ can replace $(1-\Psi)$ and the above equation will become:

$$\begin{bmatrix} (\lambda_1)^2 & \cdots & r_{1n} \\ \vdots & \ddots & \vdots \\ r_{1n} & \cdots & (\lambda_1)^2 \end{bmatrix} = \Lambda\Lambda^T$$

Accordingly, in a reduced form, we obtain the following equation:

$$\begin{bmatrix} (\lambda_1)^2 & \cdots & r_{1n} \\ \vdots & \ddots & \vdots \\ r_{1n} & \cdots & (\lambda_1)^2 \end{bmatrix} = R - \Psi = \Lambda\Lambda^T,$$

where $R-\Psi$ is a "reduced correlation matrix". If $R-\Psi$ is positive semi-definite matrix , i.e. it satisfies $R-\Psi = (R-\Psi)^T$, then this implies that $R-\Psi$ has the following spectral decomposition (i.e. a factorization into a canonical form, whereby the matrix is represented in terms of its eigenvectors to identify latent variable and corresponding eigenvalues to show strength of identified latent variable):

$$R - \Psi = UDU^T$$

In this equation, U is the matrix of eigenvectors of $R-\Psi$ and D is the diagonal matrix of corresponding eigenvalues $\Theta_1\Theta_2\ldots\Theta_n$.

$$D = \begin{bmatrix} \Theta_1 & \cdots & 0 \\ \vdots & \ddots & \vdots \\ 0 & \cdots & \Theta_n \end{bmatrix}$$

The important property of a positive semi-definite matrix is that its eigenvalues are always positive or null. Hence, $\Theta_i \geq 0$ and consequently, D can be factored into $D^{\frac{1}{2}}D^{\frac{1}{2}}$. In particular:

$$R - \Psi = \left(UD^{\frac{1}{2}}\right)\left(D^{\frac{1}{2}}U^T\right) = \Lambda\Lambda^T$$

In a general expanded form:

$$\Lambda = \left(UD^{\frac{1}{2}}\right) = \begin{bmatrix} u_{11} & \cdots & u_{1n} \\ \vdots & \ddots & \vdots \\ u_{n1} & \cdots & u_{nn} \end{bmatrix} \times \begin{bmatrix} \sqrt{\Theta_1} & \cdots & 0 \\ \vdots & \ddots & \vdots \\ 0 & \cdots & \sqrt{\Theta_n} \end{bmatrix}$$

Yet it can be observed that in the above form, Λ (or $UD^{\frac{1}{2}}$) is presented as a $n \times n$ matrix, however, as we consider here a single latent variable (the QoS within an UCS), Λ must be $n \times 1$ matrix representing $\Lambda = (\lambda_1 \lambda_2 \ldots \lambda_n)'$. Hence, from the right hand side of above equation, the largest eigenvalue Θ_i and corresponding eigenvector U_i are used for calculation of Λ , i.e., $\Lambda = U_i\sqrt{\Theta_i}$. The squared value of Λ is called communality (ζ) and can be written as:

$$\zeta = \Lambda^2 = \begin{bmatrix} (u_1)^2 \\ (u_2)^2 \\ \vdots \\ (u_n)^2 \end{bmatrix} \Theta_i$$

In the above equation, the eigenvector contains estimated unit-scaled loadings or weights (u_i) that are associated with each observed variable. The eigenvalue ζ is a shared variance among all the observed variables that represent the latent variable. Communality is obtained by multiplying squared value of u_i with ζ, which represents the relationship of latent variable with observed variable.

Coming back to the concrete example proposed in the figure 3.3 to assess the QoS of an UCS, let's assume that the communality obtained for "QoS and latency" is 0.87, when the one collected for "QoS and throughput" is 0.14. The low value received in the second case indicates a weak relationship and therefore, declares that the related breach (, i.e. throughput $<$ threshold), is insignificant and unlikely to create substantial damage.

Assessing Probability of Breach

To assess the probability of breach $P(x)$, the bot uses notion of stochastic modeling from the domain of Data Science. A stochastic model predicts a random event weighted by its probability [164]. The bot, based on the distribution model of the previous breaches $(x_{t-1}, x_{t-2}, \cdots, x_{t-n})$, suggests a stochastic model with minimum "square error" to find $P(x)$. In distribution modeling, square error as criteria with the minimum value indicates the best possible approximation (stochastic model) for the data. However, it also requires verification in terms of accuracy , i.e. how precisely a stochastic model can represent the data.

For example, during the distribution analysis, if the bot observes that *previous* breaches are lognormal increasing with minimum square error, then the probability of breach $P(x)$ is:

$$P(x) = \frac{1}{\sigma x\sqrt{2\pi}}e^{\frac{-(ln(x)-\mu)^2}{2\sigma^2}}\ ,\ if(x_{t-1},x_{t-2},\cdots,x_{t-n}) \sim LOGN(\mu,\sigma)$$

To verify the accuracy of above model, the bot performs a Paired Sample T-Test. In the test, it determines whether the mean difference between two samples, , i.e. previous breaches and random data generated using $LOGN(\mu,\sigma)$ in equation 2, is zero or not. For later case, , i.e. $\neq 0$ (when the difference between the two is not negligible), the bot dismisses the use of the expected stochastic model. This is actually the limitation of the bot.

3.2.2 Illustration: Penalization by Nexus Watchdog

This subsection presents an empirical illustration of penalizations by the bot in UCS for three HPC workflows: Redis, MongoDB, and Memcached Servers access. The HPC facility of the University of Luxembourg and Docker containers were used to emulate contractual environment of these workflows. Each of these scenarios were operated under a workload generated from the Yahoo Cloud Service Benchmark (YCSB) [165] which was deployed to continuously monitor the QoS of the system in terms of throughput (operations per second), read latency (time to read data from database), and update latency (time to update data in database). For the experiments described in the sequel, the input parameters given to be passed to the YCSB benchmark for evaluation correspond to the different number of operations (ranging from 0 to 10,000), an increasing number of records (ranging from 0 to 10,000), and a number of threads ranging from 0 to 100. Python (for scripting) and R (for data visualization) were used to identify the smart contract breach, in which case the bot was activated to request penalization. In addition, several data analysis tools were used to assist the PFM analysis such as Arena Input analyzer, STATA or IBM Statistical Analysis Software Package (SPSS).
Figure 3.4 presents YCSB monitoring of service providers in terms of unit-scaled throughput, read latency and update latency. The YCSB data of all three service providers was used by the bot to calculate communality for throughput (0.38), read latency (0.46), and update latency (0.33). It can be observed that read latency has highest value and consequently, the strongest relationship with QoS. Therefore, the related breach, , i.e. read latency $>$ threshold, is significant and most likely to create substantial damage.

For each workflow, the following operations were performed: (a) the threshold was set to average read latency, which was calculated from its YCSB data, (b) based on the condition, , i.e. read latency $>$ average read latency, previous breaches $(x_{t-1},x_{t-2},\cdots,x_{t-n})$ were identified, (c) distribution modeling of previous breaches was performed, and (d) stochastic model with minimum square error was identified and further verified for accuracy using Paired Sample T-Test. The stochastic models for read latency of Redis and Memcached successfully passed the T-Test. However, for MongoDB (as it failed the prior T-Test) the procedure in preceding paragraph was repeated for throughput (with second highest communality value of 0.38) and stochastic model identified successfully passed the T-Test.

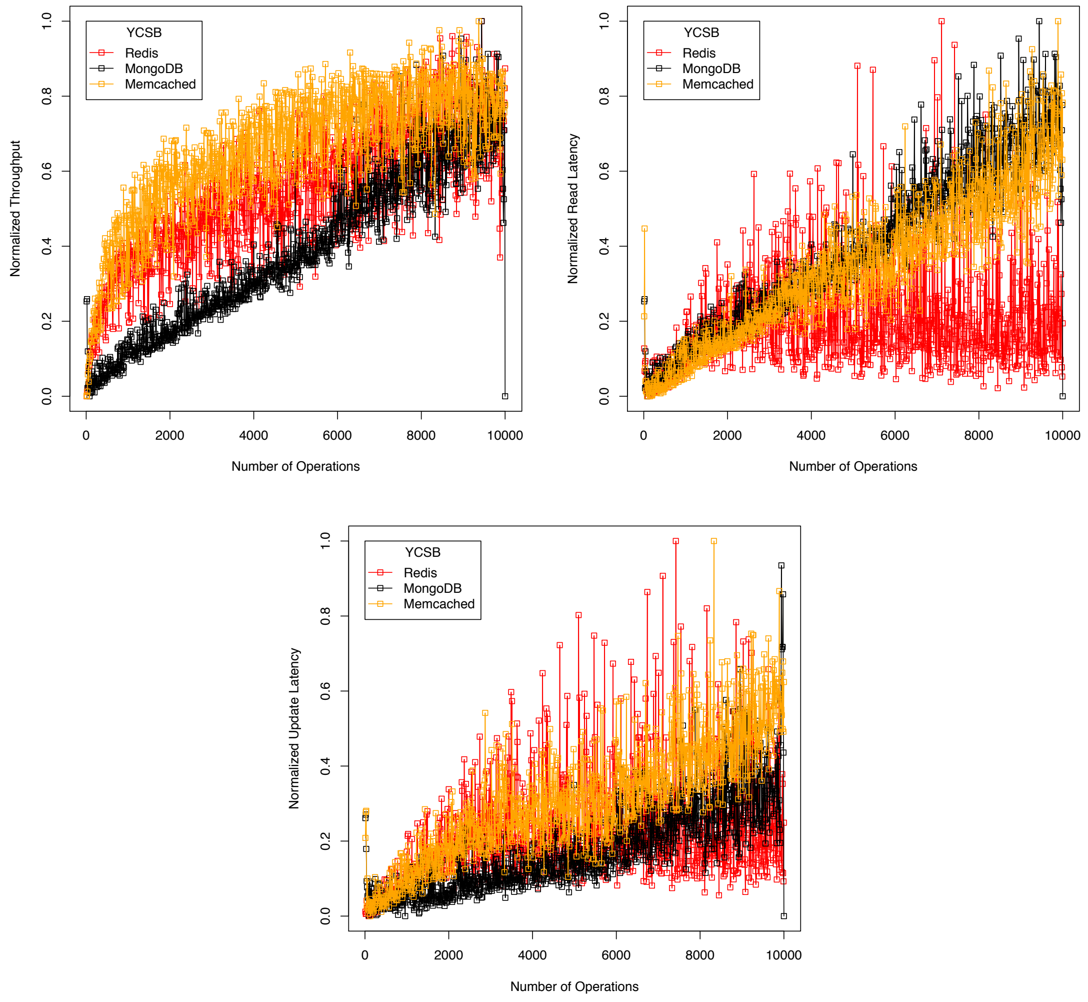

Figure 3.4: YCSB (version 0.12.0) Monitoring of Redis, MongoDB, and Memcached

The tables 3.2 and 3.3 present the implementation and results of the PFM analysis conducted within the NESUS watchdog for the considered workflows. For instance, the top figures shows previous breaches based on two conditions: "read latency $>$ average read latency" for Redis and Memcached, and "throughput $<$ average throughput" for MongoDB. The obtained distribution models are exhibited in each case, as well as the parameters of the stochastic models. It can be observed that for Redis and Memecached, previous breaches in read latency are lognormal increasing and for MongoDB, previous breaches in throughput are beta increasing. We propose within each HPC workflow the measured square error (Redis: 0.007417, Memcashed: 0.003444, and MongoDB : 0.018634). Moreover, as p-values of Paired Sample T-Test (Redis: 0.5449, Memcashed: 0.8258, and MongoDB: 0.4788) are greater than 0.05, the null hypothesis (the two samples are same) is accepted as compared to alternate hypothesis (the two samples are different). Hence, the stochastic models for Redis (read latency) , i.e. $0.12 + LOGN(0.204, 0.117)$, Memcached (read latency) , i.e. $0.27 + LOGN(0.245, 0.137)$, and MongoDB (throughput) , i.e. $-0.48 + 0.17 * BETA(2.49, 1.48)$, can be used by PFM to find probability of breach $P(x)$. In

Table 3.2 NESUS Watchdog (a software bot) - Stochastic Models and Penalization for the Redis and Memcached workflows.

Redis	**Memcached**
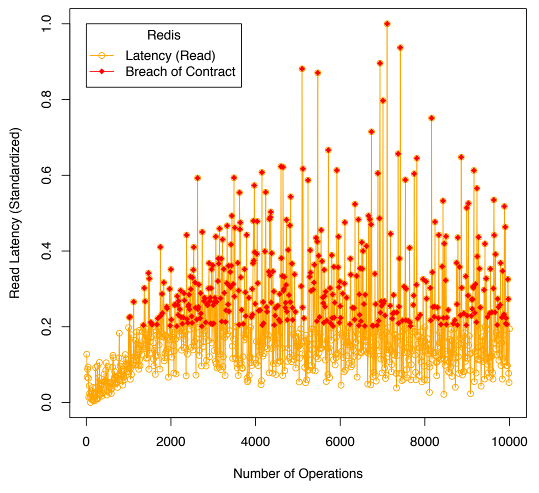	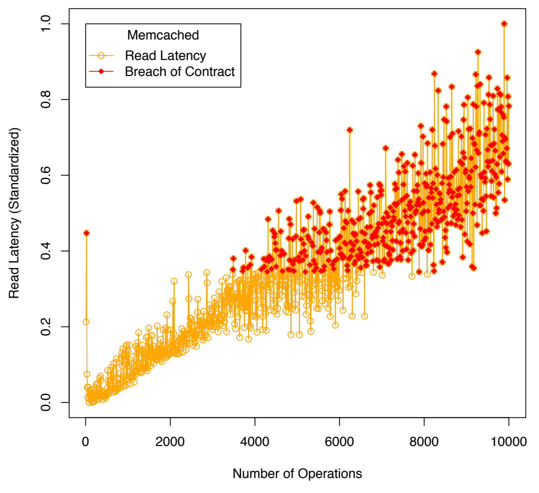
Distribution: Lognormal **Stochastic Model:** $0.12 + LOGN(0.204, 0.117)$	**Distribution:** Lognormal **Stochastic Model:** $0.27 + LOGN(0.245, 0.137)$
Square Error: 0.007417 p-value (t-test): $0.5449 (> 0.05)$ Equation: $P(x) = \left\{ \frac{1}{\sigma x\sqrt{2\pi}} e^{\frac{-(ln(x)-\mu)^2}{2\sigma^2}} \right.$	Square Error: 0.003444 p-value (t-test): $0.8258 (> 0.05)$ Equation: $P(x) = \left\{ \frac{1}{\sigma x\sqrt{2\pi}} e^{\frac{-(ln(x)-\mu)^2}{2\sigma^2}} \right.$
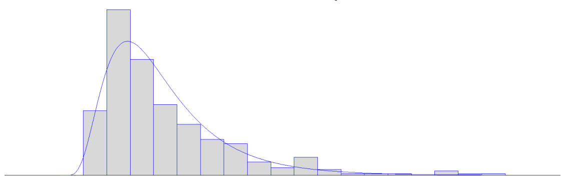	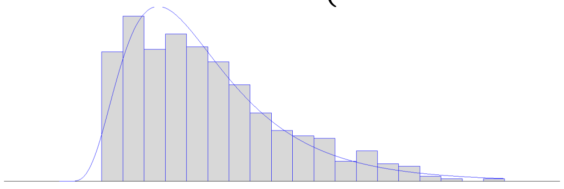

Penalization

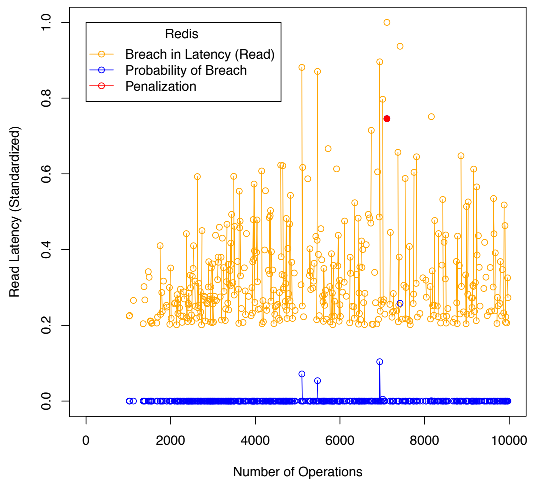	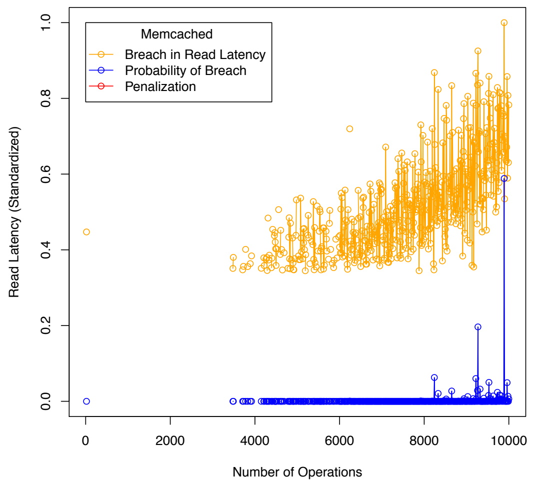

Table 3.3 NESUS Watchdog (a software bot) - Stochastic Models and Penalization for the MongoDB workflow.

MongoDB	
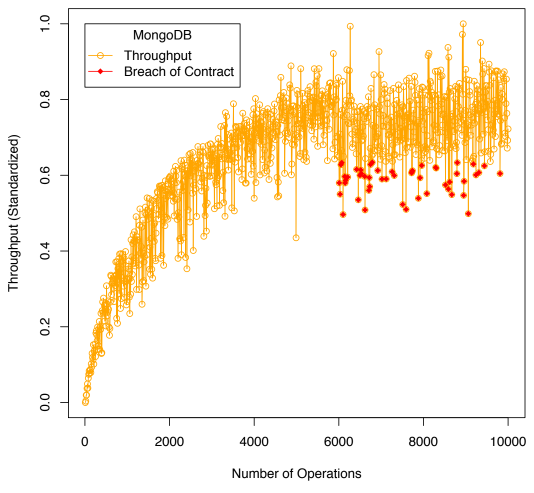 **Distribution:** Beta **Stochastic Model:** $0.48+0.17*BETA(2.49,1.48)$	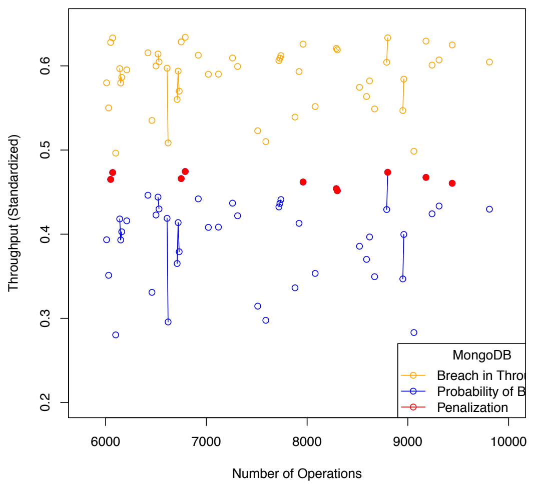 **Penalization**
Square Error: 0.018634 p-value (t-test): $0.4788(>0.05)$ Equation: $P(x)=\left\{\frac{x^{\beta-1}(1-x)^{\alpha-1}}{\int_0^1 t^{\beta-1}(1-t)^{\alpha-1}dt}\right.$ 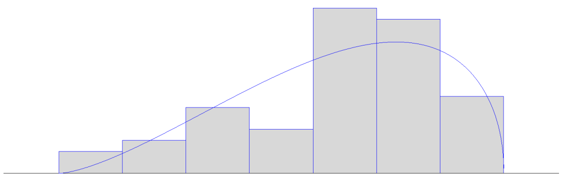	

particular, it was demonstrated a lognormal $P(x)$ for Redis and Memcached and beta $P(x)$ for MongoDB.

Penalization aspects are also illustrated. For Redis and Memcached, the penalization request was issued by the bot based on the condition: $P(x) > 0.70$, whereas, for MongoDB the condition was: $P(x) > 0.45$. It can be observed that only Redis and MongoDB Servers were penalized. Technically, this difference could be attributed to the fact that Memcached is simply used for caching and therefore, it is less prone to breach of contract. Whereas, Redis and MongoBD as databases and message brokers are performing more complex operations and are more likely to cause a breach.

3.3 Conclusion

Due to their scale and the wide range of possible applications and involved technologies, UCS requires adapted frameworks to enable resilient and secure executions.

In this chapter, we have reviewed the general concepts of faults, fault tolerance and robustness before detailing the main approaches suitable for large scale HPC systems. New opportunities and challenges have been highlighted, in particular at the level of hardware, network, MPI resilience. Novel data structures based on DLT have been introduced as a new field worth further investigations for large-scale experiments and validations. An potential illustration on regulatory compliance within UCS has been proposed.

What emerges is the need for the apparition of additional disruptive paradigms and solutions at all levels: from hardware, languages, compilers, operating systems, middleware, services, and application-level solutions. In this aspects, there are several research challenges for resilience in Ultrascale systems that should be faced in a near future:

Characterization of hardware and software faults in Ultrascale systems Characterization of hardware and software faults is essential for making informed choice about research needs for the resilience of Ultrascale systems. From the hardware perspective if silent hardware faults are exceedingly rare, then the hard problem of detecting such errors in software or tolerating their impact can be ignored. If errors in storage are exceedingly rare, while errors in compute logic are frequent, then research on mechanisms for hardening data structures and detecting memory corruptions in software is superfluous.

Development of a standardized fault-handling model Development of a standardized fault-handling model is key to providing guidance to application and system software developers about how they will be notified about a fault, what types of faults they may be notified about, and what mechanisms the system provides to assist recovery from the fault. Applications running on today?s high performance computing systems are not even notified of faults or given options as to how to handle faults. If the application happens to detect an error, the computer may also eventually detect the error and kill the application automatically, making application recovery problematic.

Improved fault prediction, containment, detection, notification, and recovery Scale is a major opportunity for applications Ultrascale computing Systems. However, the larger the scale, the higher the probability of a failure in some part of the system. To build such a systems, resilience is a must, and that means the we need better fault prediction mechanisms, containment measures and recovery from failures to allow the applications keep-on working even if a specific component fails. [**?**]

Programming abstractions for resilience in Ultrascale systems Programming abstractions for resilience will be able to grow out of a standardized fault handling model. Several programming abstractions will need to be developed and supported in order to develop resilient Ultrascale applications. The development of fault-tolerant algorithms requires various resilience services.

Standardized evaluation of fault-tolerance approaches Standardized evaluation of fault tolerance approaches will provide a way to measure the efficiency of a new approach compared with other known approaches. It will also provide a way to measure the effectiveness of an approach on different architectures and at different scales. The latter will be important to determine whether the approach can scale to serve the needs of Ultrascale systems.

Offering a global view on the reliability/resilience issues will allow to define the right level of information exchange between all layers and components in order to have global (cross-layer/component) solution.